RIA-77-U1030

Cy No. 1

OPTIMAL CONTROL OF ACTIVE RECOIL MECHANISMS

BY

S. M. WU

A. N. MADIWALE

February 1977

TECHNICAL REPORT

Prepared By

University of Wisconsin-Madison
Madison, Wisconsin 53706

Prepared For

ENGINEERING DIRECTORATE

&

GENERAL THOMAS J. RODMAN LABORATORY

ROCK ISLAND ARSENAL
ROCK ISLAND, ILLINOIS 61201

UNCLASSIFIED

SECURITY CLASSIFICATION OF THIS PAGE *(When Data Entered)*

REPORT DOCUMENTATION PAGE		READ INSTRUCTIONS BEFORE COMPLETING FORM
1. REPORT NUMBER R-TR-77-024	2. GOVT ACCESSION NO.	3. RECIPIENT'S CATALOG NUMBER
4. TITLE *(and Subtitle)* Optimal Control of Active Recoil Mechanisms		5. TYPE OF REPORT & PERIOD COVERED Final June 1976 - December 1976 6. PERFORMING ORG. REPORT NUMBER
7. AUTHOR(s) S.M. Wu A.N. Madiwale		8. CONTRACT OR GRANT NUMBER(s) DAAA09-76-M-2017
9. PERFORMING ORGANIZATION NAME AND ADDRESS University of Wisconsin-Madison Mechanical Engineering Department Madison, Wisconsin		10. PROGRAM ELEMENT, PROJECT, TASK AREA & WORK UNIT NUMBERS 1W161102AH55
11. CONTROLLING OFFICE NAME AND ADDRESS Engineering Directorate/Ware Simulation Division Rock Island Arsenal Rock Island, IL 61201		12. REPORT DATE February 1977 13. NUMBER OF PAGES 80
14. MONITORING AGENCY NAME & ADDRESS *(if different from Controlling Office)*		15. SECURITY CLASS. *(of this report)* UNCLASSIFIED 15a. DECLASSIFICATION/DOWNGRADING SCHEDULE

16. DISTRIBUTION STATEMENT *(of this Report)*

Approved for public release, distribution unlimited.

17. DISTRIBUTION STATEMENT *(of the abstract entered in Block 20, if different from Report)*

18. SUPPLEMENTARY NOTES

19. KEY WORDS *(Continue on reverse side if necessary and identify by block number)*

1. Recoil Mechanism
2. Feedback
3. Optimal Control
4. Servovalve
5. Objective Function
6. Breech Force
7. Rod Pull
8. Non-linear Optimization

20. ABSTRACT *(Continue on reverse side if necessary and identify by block number)*

A servo-valve feedback system with variable control law is proposed for modification of a conventional hydropneumatic recoil mechanism to minimize peak recoil force for any round fired. Phase-plane-delta method of digital simulation is used to simulate the recoil mechanism model. An objective function with direct physical interpretations is developed and non-linear optimization techniques are used to design feedback gains for each firing round. The method is applied to M37 recoil mechanism and significant improvement in recoil force trajectories is obtained.

DD FORM 1 JAN 73 1473 EDITION OF 1 NOV 65 IS OBSOLETE

UNCLASSIFIED

SECURITY CLASSIFICATION OF THIS PAGE *(When Data Entered)*

FOREWORD

This report was prepared by Prof. S. M. Wu and Mr. A. N. Madiwale of the University of Wisconsin-Madison in compliance with Contract No. DAAA09-76-M-2017. This work was performed for the Ware Simulation Division, Engineering Directorate, and the Research Directorate, GEN Thomas J. Rodman Laboratory, Rock Island, Illinois, with Mr. R. E. Kasten as Project Engineer

ACKNOWLEDGEMENT

This work was supported by the Ware Simulation Division, Engineering Directorate, Rock Island Arsenal, Rock Island, Illinois under Contract No. DAAA09-76-M-2017.

The authors developed their basic understanding of modeling recoil mechanisms through reports by Nerdahl and Frantz (8, 9, 10) and personal communications with the Ware Simulation Division. The suggestions by and discussions with Mr. Robert J. Radkiewicz and Mr. Robert E. Kasten of the Ware Simulation Division were very helpful and are deeply appreciated.

TABLE OF CONTENTS

LIST OF FIGURES

LIST OF TABLES

NOTATION

A_R - Recoil rod area. in^2

A_C - Control rod area. in^2

A_D - Floating piston area. in^2

A_N - Total area of floating piston = $A_C + A_D$. in^2

A_1 - Area of orifice between recoil and recuperating chamber. in^2

A_2 - Area of orifice between recuperating and control chamber. in^2

$A_3(x)$ - Variable area of the groove in the floating piston at position x. in^2

$B(t)$ - Breech force at time t. lbf

C_1 - Discharge coefficient for orifice A_1.

C_2 - Discharge coefficient for orifice A_2.

C_3 - Discharge coefficient for orifice A_3.

C_q - Equivalent friction coefficient for frictional loss at orifices

F_R - Dry friction at recoil piston.

F_P - Dry friction at floating piston.

F_q - Equivalent dry friction.

g_1 - Position feedback gain.

g_2 - Velocity feedback gain.

g_3, g_4 - other feedback gains for nonlinear feedback.

J - objective function

J_1

J_2

J_3 } - Components of objective function

J_4

J_5

m_p - Mass of the floating piston lbf sec^2/in

m_R - Mass of the recoiling parts lbf sec^2/in

m_q - Equivalent mass lbf sec^2/in

P_0 - Initial gas pressure lbf/in^2

P_G - Gas pressure at time t lbf/in^2

R - Gas constant

RDPL(t) - Rod pull at time t lbf

RDPLD(t) - Desired Rod pull at time t lbf

T - Recoil time sec

U(t) - Open area of servo valve in^2

x - Position of recoiling parts with respect to recoil rod in

$\dot{x}$ - Velocity of recoiling parts with respect to recoil rod in/sec

$\ddot{x}$ - Acceleration of recoiling parts

y - Position of floating piston with respect to recoiling parts

w - Total weight of the recoiling parts.

w_q - Equivalent weight of recoiling parts.

w_1
w_2
w_3
w_4
} - Weighting factors for components in the objective function.

α - The angle of elevation of the gun barrel radians

ρ - Mass density of the hydraulic fluid.

SUMMARY

Mathematical model for a conventional hydro-pneumatic recoil mechanism is developed from physical laws. This mathematical model is simulated on a digital computer by Phase-Plane-Delta method. The time histories of all pertinent parameters such as position of recoiling parts, hydraulic pressures in different chambers, rod pull are available and can be plotted.

A linear state feedback control system is proposed to adapt this conventional recoil mechanism to perform satisfactorily for all firing zones. The control and optimization problem is formulated. An objective function with direct relations to the performance and constraints of the problem is formulated. Davidon-Fletcher-Powell variable metric method of nonlinear optimization is used to design the feedback gains of the state feedback control law.

The above optimization procedure is applied to M-37 recoil mechanism for zone 5 through 8. This recoil mechanism originally was designed for zone 7. One set of feedback gains is designed for each zone and switching of control laws is suggested. A significant improvement in the recoil force time trajectory shape and reduction in peak force of 2.5 to 25 percent is obtained.

INTRODUCTION

Recoil mechanisms dissipate energy of the reaction of gunfire at a controlled rate so as to minimize the recoil force transferred to the carriage of a weapon system without exceeding available recoil length. Nerdahl and Frantz [9] have developed three degrees of freedom nonlinear models of hydropneumatic recoil mechanisms and a procedure to design a variable area orifice to control the energy dissipation. The procedure defines a control function or desired control recoil force-time trajectory for a design firing charge and with the help of digital simulation of the model, computes the orifice area at different positions of the recoil mechanism. This design performs satisfactorily for the designated firing charge, but far from optimum for other firing charges. Thus, a control system which can adapt to different firing zones is desirable.

A linear state feedback control system with variable gains is proposed in the report. A separate control law is designed for each firing charge and the control law corresponding to the charge being fired is selected from this predesigned set. This control scheme can be implemented by adding a servo valve operating in

tandem with the variable area orifice. The feedback gains for the servo valve can be selected from a predesigned set by identifying the charge being fired by sensing signals such as acceleration with the help of a microprocessor or special purpose digital electronics.

The design of the optimal control law is complicated by the highly nonlinear nature of the model induced by turbulent flow through orifices, dry friction at piston-cylinder surfaces and adiabatic gas compression. The nonlinear second order model is simulated on a digital computer using Phase-plane-delta method. A multifactor objective function with direct physical interpretation is developed as a function of the variables computed in the simulation. Davidon-Fletcher-Powell variable metric quasi-Newton nonlinear optimization algorithm is used to minimize the objective function. The procedure is applied to a M-37 105 mm recoil mechanism. Also, velocity feedback for lower zones 1, 5, and 6 is evaluated.

I

MATHEMATICAL MODEL FOR HYDROPNEUMATIC RECOIL MECHANISM

A schematic diagram for a conventional hydropneumatic recoil mechanism is shown in Fig. 1. A mathematical model based on the physical laws is developed with the following assumptions.

1) Flow through orifices is a potential flow.
2) Temperature variations do not affect the discharge coefficients for the orifice.
3) The recoil mechanism is secured to the carriage through a rigid link called the rod and the carriage rests on a rigid support.
4) Only translation of the recoil parts in direction of firing is considered.
5) There is no cavitation in any chamber.

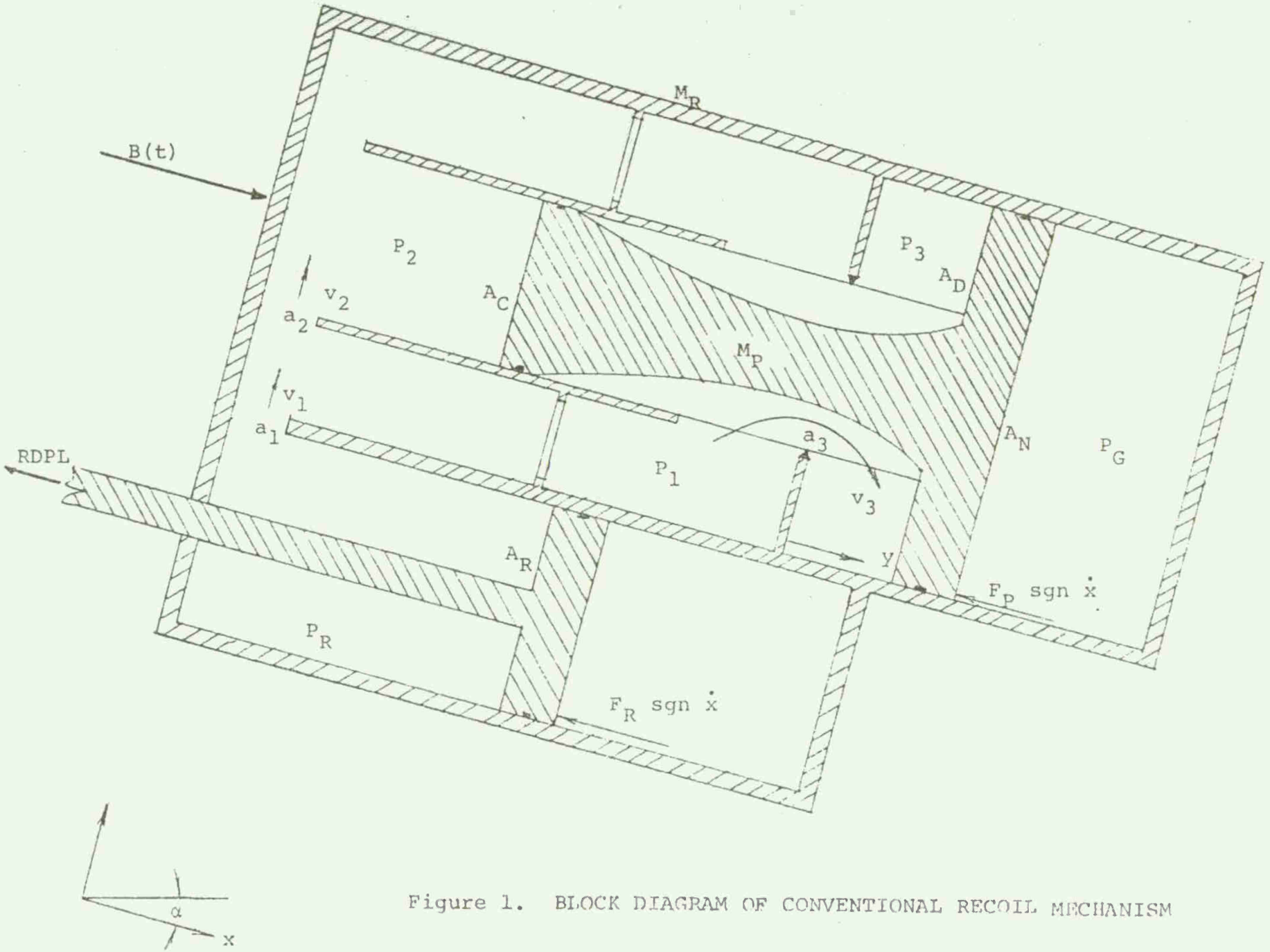

Figure 1. BLOCK DIAGRAM OF CONVENTIONAL RECOIL MECHANISM

PRESSURE RELATIONS

$$P_R - P_1 = \left(\frac{\rho}{2}\right) \left(\frac{A_R}{A_1 C_1}\right)^2 \dot{x}^2 \, \text{sgn}\dot{x}$$

$$= T_1 \dot{x}^2 \, \text{sgn} \, \dot{x} \qquad (1)$$

where $T_1 = \left(\frac{\rho}{2}\right) \left(\frac{A_R}{A_1 C_1}\right)^2$

$$P_1 - P_2 = \left(\frac{\rho}{2}\right) \left(\frac{A_C}{A_2 C_2}\right)^2 \dot{y}^2 \, \text{sgn}\dot{y}$$

$$= \left(\frac{\rho}{2}\right) \left(\frac{A_C A_R}{A_2 C_2 A_N}\right)^2 \dot{x}^2 \, \text{sgn} \, \dot{x}$$

$$= T_2 \dot{x}^2 \, \text{sgn} \, \dot{x} \qquad (2)$$

where $T_2 = \left(\frac{\rho}{2}\right) \left(\frac{A_C A_R}{A_2 C_2 A_N}\right)^2$

$$P_1 - P_3 = \left(\frac{\rho}{2}\right) \left(\frac{A_D}{C_3 A_3}\right)^2 \dot{y}^2 \, \text{sgn}\dot{y}$$

$$= \left(\frac{\rho}{2}\right) \left(\frac{A_D A_R}{C_3 A_3 A_N}\right)^2 \dot{x}^2 \, \text{sgn}\dot{x}$$

$$= T_3 \dot{x}^2 \, \text{sgn} \, \dot{x} \qquad (3)$$

where $T_3 = \left(\frac{\rho}{2}\right) \left(\frac{A_D A_R}{C_3 A_3 A_N}\right)^2$

The gas pressure relation

$$P_G = P_0 \left(\frac{V_0}{V_0 - A_R x}\right)^R \qquad (4)$$

Thus the pressure equations are

$$P_R = P_1 + T_1 \dot{x}^2 \operatorname{sgn} \dot{x} \qquad (1)$$

$$P_2 = P_1 - T_2 \dot{x}^2 \operatorname{sgn} \dot{x} \qquad (2)$$

$$P_3 = P_1 - T_3 \dot{x}^2 \operatorname{sgn} \dot{x} \qquad (3)$$

$$P_G = P_0 \left(\frac{V_0}{V_0 - A_R x}\right)^R \qquad (4)$$

Force balance for floating piston

$$m_p\left(1 + \frac{A_R}{A_N}\right) \ddot{x} = m_p g \sin \alpha + A_D P_3 + A_C P_2 - A_N P_G - F_p \operatorname{sgn} \dot{x} \qquad (5)$$

Substituting for P_R, P_2, P_3 and P_G from equations 1, 2, 3, & 4 in 5 we have

$$m_p\left(1+\frac{A_R}{A_N}\right) \ddot{x} = m_p g \sin \alpha + A_D(P_1 - T_3 \dot{x}^2 \operatorname{sgn}\dot{x}) + A_C(P_1 - T_2 \dot{x}^2 \operatorname{sgn}\dot{x}) - A_N P_0 \left(\frac{V_0}{V_0 - A_R x}\right)^R - F_p \operatorname{sgn}\dot{x}$$

$$= m_p g \sin \alpha - (A_D T_3 + A_C T_2) \dot{x}^2 \operatorname{sgn}\dot{x} + (A_D + A_C) P_1 + m_p g \sin \alpha - A_N P_0 \left(\frac{V_0}{V_0 - A_R x}\right)^R - F_p \operatorname{sgn}\dot{x}$$

$$A_N P_1 = m_p\left(1+\frac{A_R}{A_N}\right)\ddot{x} - m_p g \sin\alpha - (A_D T_3 + A_C T_2)\dot{x}^2 \operatorname{sgn}\dot{x}$$

$$+ A_N P_0 \left(\frac{V_0}{V_0 - A_R x}\right)^R + F_p \operatorname{sgn}\dot{x} \tag{6}$$

Force balance for recoil mass

$$m_R\ddot{x} = B(t) + m_R g \sin\alpha - A_D P_3 - A_C P_2 + A_N P_G$$

$$+ F_p \operatorname{sgn}\dot{x} - A_R P_R - F_R \operatorname{sgn}\dot{x} \tag{7}$$

Adding Equations (5) and (7) we have

$$\left[m_R + m_p\left(1+\frac{A_R}{A_N}\right)\right]\ddot{x} = (m_p+m_R) g \sin\alpha + B(t) -$$

$$A_R P_R - F_R \operatorname{sgn}\dot{x} \tag{8}$$

Substituting for P_1 in Eq. (8) from Eq. (6) we have

$$\left[m_R + m_p\left(1+\frac{A_R}{A_N}\right)\right]\ddot{x} = (m_p + m_R) g \sin\alpha + B(t)$$

$$-F_R \operatorname{sgn}\dot{x} - A_R T_1 \dot{x}^2 \operatorname{sgn}\dot{x} - \frac{A_R}{A_N}\left[m_p\left(1+\frac{A_R}{A_N}\right)\ddot{x} - m_p g \sin\alpha\right.$$

$$\left. + (A_C T_2 + A_D T_3)\dot{x}^2 \operatorname{sgn}\dot{x} + A_N P_0 \left(\frac{V_0}{V_0 - A_R x}\right)^R + F_p \operatorname{sgn}\dot{x}\right]$$

$$= \left[m_R + m_p\left(1+\frac{A_R}{A_N}\right)\right] g \sin\alpha + B(t) - \left(F_R + F_p \frac{A_R}{A_N}\right)\operatorname{sgn}\dot{x}$$

$$- \left[A_R T_1 + \frac{A_R}{A_N}(A_C T_2 + A_D T_3)\right]\dot{x}^2 \operatorname{sgn}\dot{x} - A_R P_0 \left(\frac{V_0}{V_0 - A_R x}\right)^R$$

$$- \frac{A_R}{A_N} m_p\left(1+\frac{A_R}{A_N}\right)\ddot{x}$$

Finally

$$[m_R+m_p(1+\frac{A_R}{A_N})^2]\ddot{x} + [A_RT_1+\frac{A_R}{A_N}(A_CT_2+A_DT_3)]\dot{x}^2\ sgn\dot{x}$$

$$+ A_RP_0(\frac{V_0}{V_0-A_Rx})^R + (F_R+F_p\frac{A_R}{A_N})\ sgn\dot{x}$$

$$=[m_R+m_p(1+\frac{A_R}{A_N})]g\ \sin\alpha + B(t) \qquad (9)$$

Let

m_q - equivalent mass

$$= m_R + m_p\ (1 + \frac{A_R}{A_N})^2$$

C_q - equivalent damping coeffienct

$$= [A_RT_1 + \frac{A_R}{A_N}\ (A_CT_2 + A_DT_3)]$$

F_q - equivalent dry friction

$$= (F_R + F_p\ \frac{A_R}{A_N})$$

W_q - equivalent weight

$$= [m_R + m_p\ (1 + \frac{A_R}{A_N})]\ g\ \sin\alpha$$

Thus equation (9) can be rewritten as

$$m_q\ddot{x} + C_q\dot{x}^2 sgn\dot{x} + F_q sgn\dot{x} + A_RP_0(\frac{1}{1 - \frac{A_R}{V_0}x})^R$$

$$= W_q + B(t) \qquad (10)$$

Note - C_q is not a constant and is a function of the position of the floating piston due to the variable orifice area A_3.

The rod pull is

$$RDPL = P_R A_R + F_R \operatorname{sgn}\dot{x} \tag{11}$$

From equations (8) and (11) we have

$$RDPL = -[m_R + m_p(1+\frac{A_R}{A_N})]\ \ddot{x} + (m_p+m_R)g \sin\alpha + B(t) \tag{12}$$

Thus equation (10) is the final model of the form

$$m\ddot{x} + (a+f(x))\dot{x}^2 \operatorname{sgn}\dot{x} + k(1-a_0 x)^{-R} = W + B(t)$$

and equations 1, 2, 3, 4, and 12 are relations for all pertinent variables.

II

DIGITAL SIMULATION OF RECOIL MECHANISM MODEL

The nonlinear second order model developed in Section I Equation (10) can be simulated on a high speed digital computer by phase-plane-delta method. This method transforms a forced nonlinear model into a linear oscillator for a short interval of time and is explained in detail in Appendix I. The simulation results in time histories of all the pertinent variables such as position, velocity, rod pull, and all the pressures. This method is computationally very efficient.

The model in equation (10) can be reformulated in phase-plane-delta format as follows

$$m_q\ddot{x} + c_q\dot{x}^2\mathrm{sgn}\dot{x} + A_R P_0\left(1-\frac{A_R}{V_0}x\right)^{-R} + F_q\mathrm{sgn}\dot{x} = W_q + B(t)$$

or

$$\ddot{x} + p^2(x + \delta x) = 0 \tag{13}$$

where

$$\delta x = -x + \frac{1}{p^2 m_q}\left\{C_q\dot{x}^2\mathrm{sgn}\dot{x} + A_R P_0\left(1-\frac{A_R}{V_0}x\right)^{-R} + F_q\mathrm{sgn}\dot{x} - W_q - B(t)\right\} \tag{14}$$

From initial conditions $x_0 = 0$, $\dot{x}_0 = 0$, the simulation is started and run until the recoil mechanism starts counter-recoil.

A fortran program is written to simulate the recoil

mechanism based on equations (13) and (14).

An example simulation was run for M-37 recoil mechanism zone 7 firing charge. The phase plane, x, $\dot{x}$, P_3, P_G, and rod pull are plotted in Figures 2, 3, 4, 5, 6, and 7.

The simulation results are in agreement with a digital simulation run by the Ware Simulation Division at Rock Island Arsenal using Continuous System Modeling Program (CSMP).

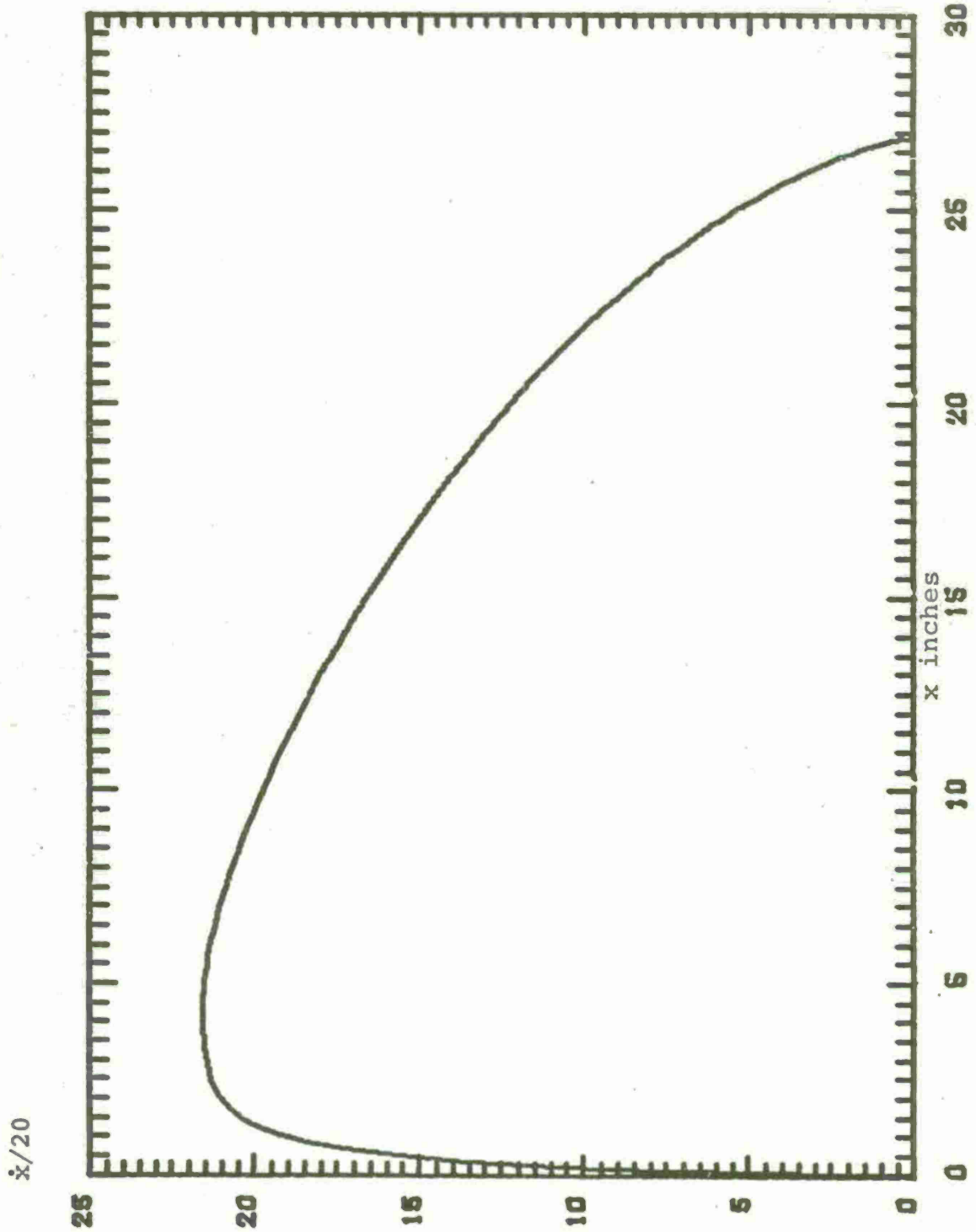

Figure 2 Phase plane for Zone 7

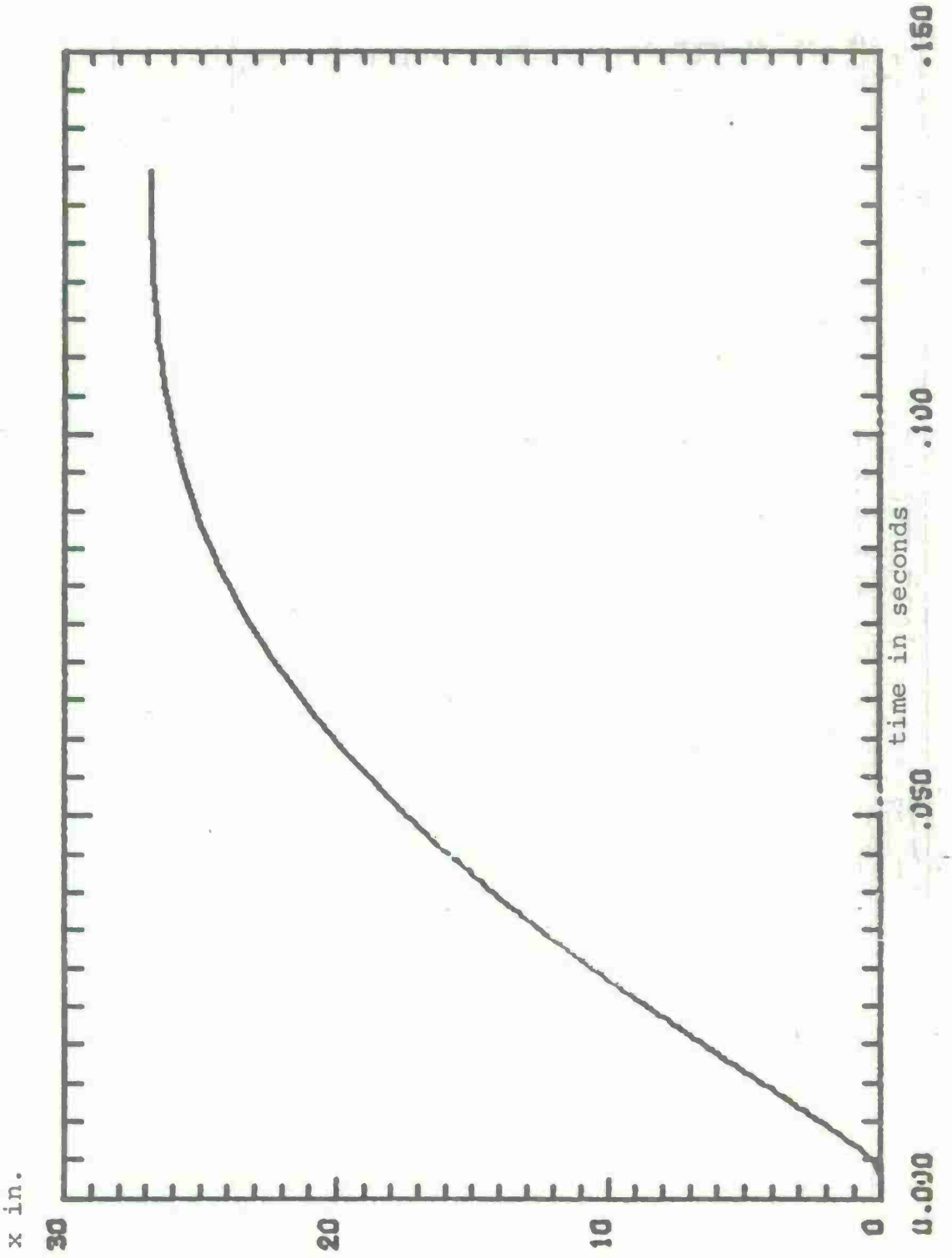

Figure 3 Displacement for Zone 7

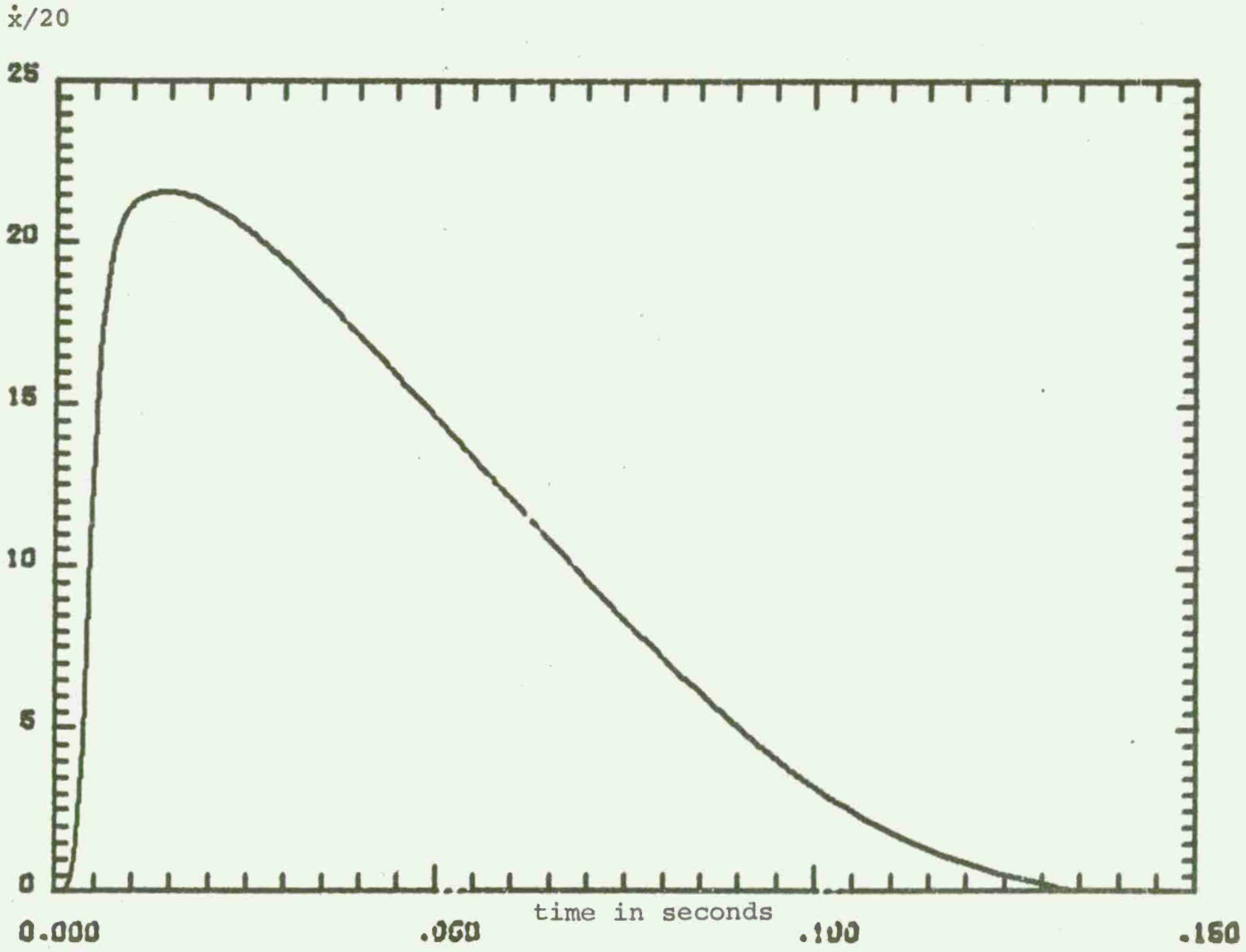

Figure 4 Velocity for Zone 7

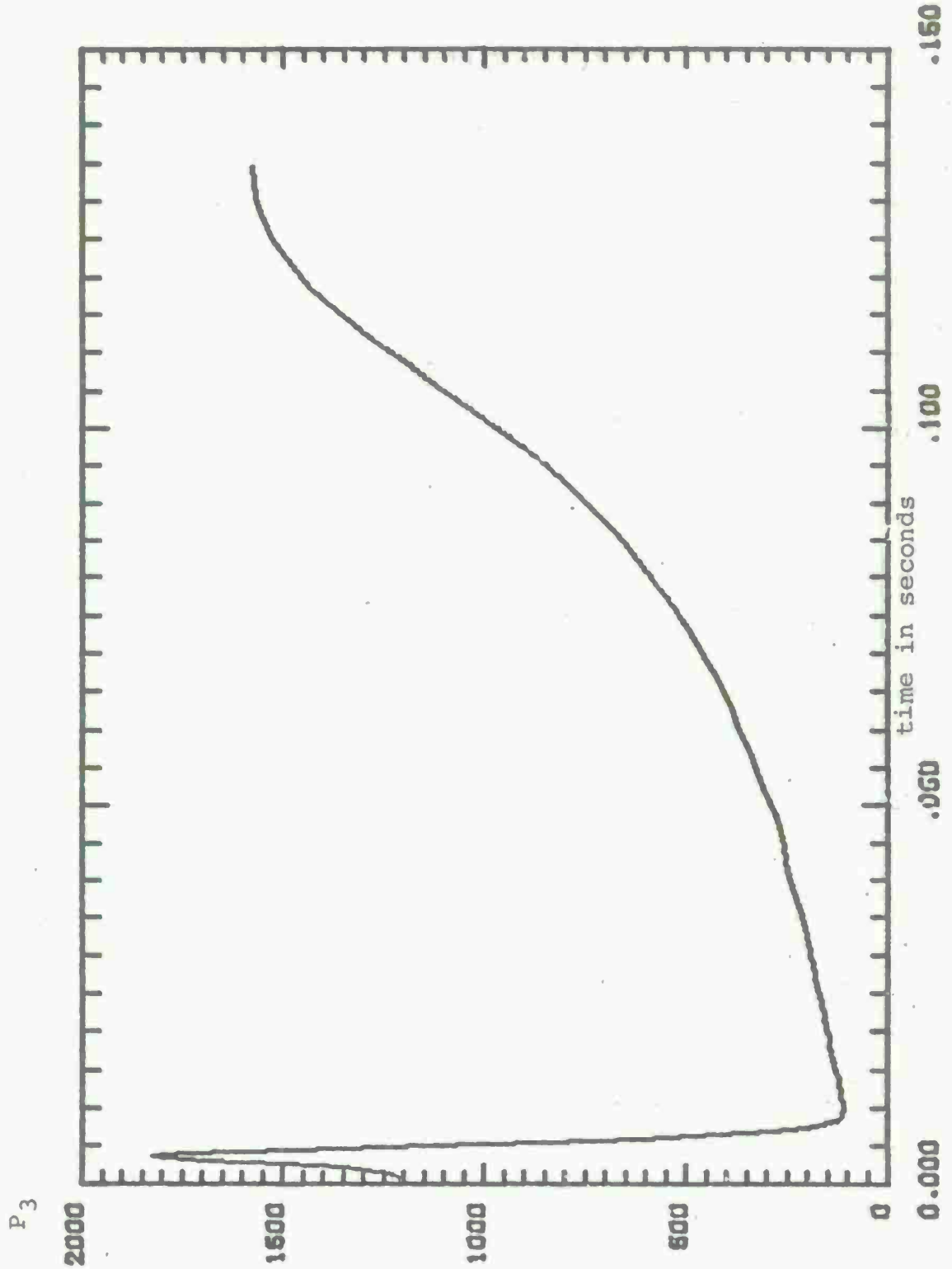

Figure 5 Cavitation Pressure for Zone 7

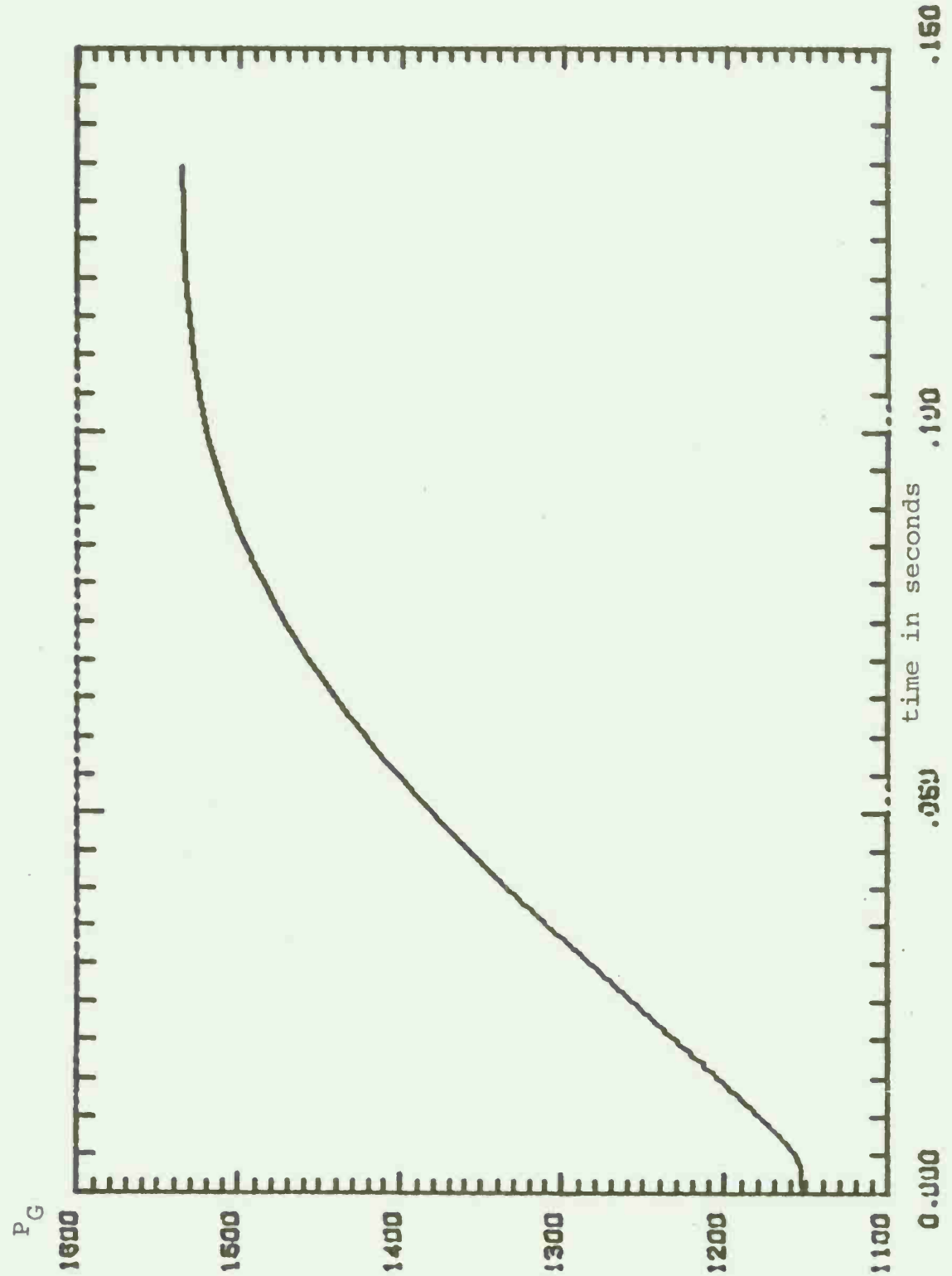

Figure 6 Gas Pressure for Zone 7

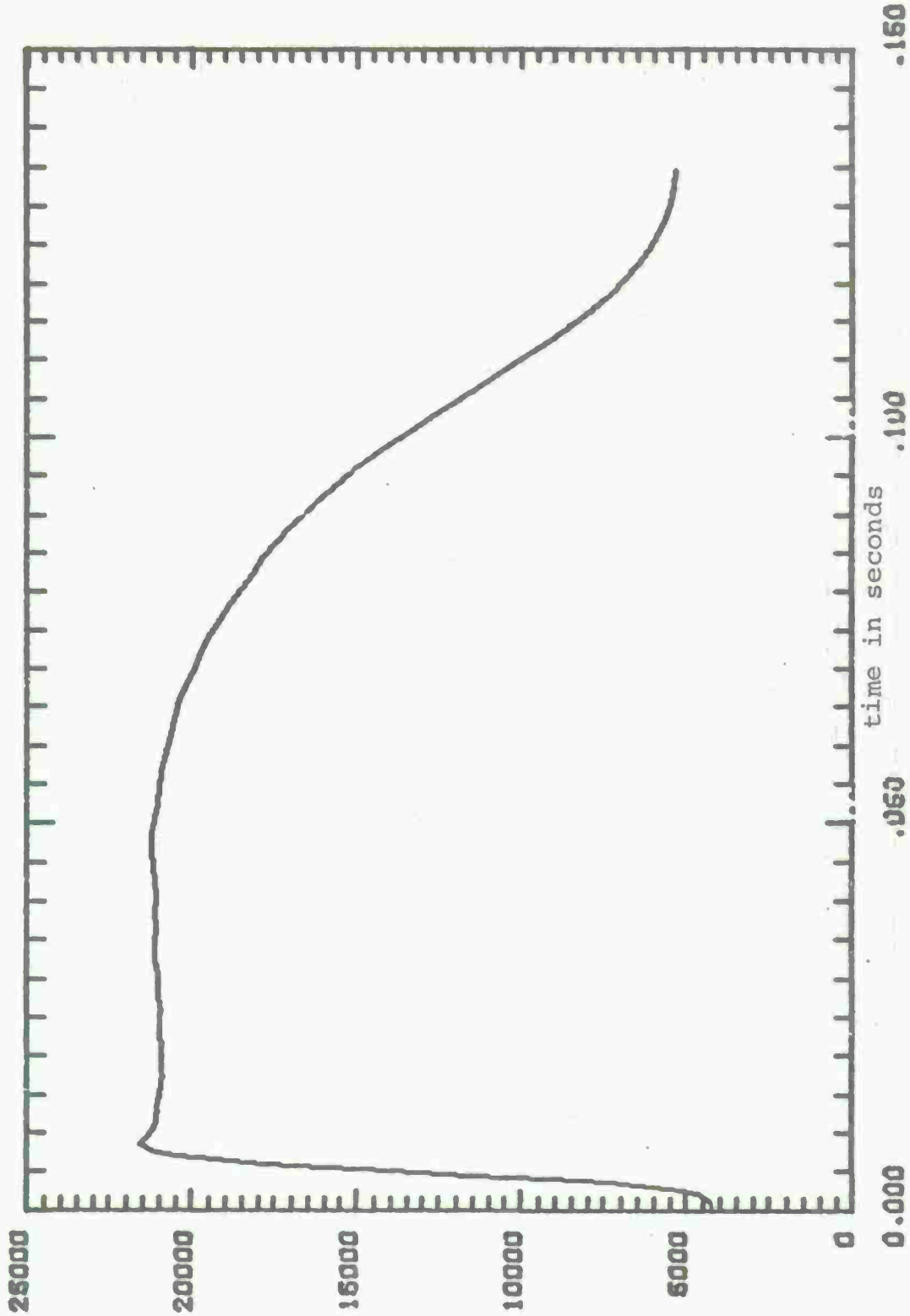

Figure 7 Rod Pull for Zone 7

III

FORMULATION OF ADAPTIVE CONTROL AND OPTIMIZATION PROBLEM

The control groove machined in the floating piston is designed for a designated zone and performs satisfactorily when used for the design zone. The purpose of this research is to adapt the recoil mechanism such that it adapts to the charges being fired so as to perform satisfactorily without violating the system constraints. A modified design of the recoil mechanism with a servo valve operating in tandem with the variable area groove is shown in Figure 8. The area of the servo valve that is open for the flow of hydraulic fluid is controlled by a feedback law. The feedback law can be changed by sensing the zone being fired. This adds the flexibility to change and adapt to the firing zone.

3.1 Linear State Feedback

A linear state feedback control is proposed to control the area of the servo valve and is of the form

$$u = g_1 x + g_2 \dot{x} \tag{15}$$

where g_1 and g_2 are feedback gains and u is the area of the servo valve. The corresponding modification in the mathematical model is in the equivalent damping coefficient C_q as follows

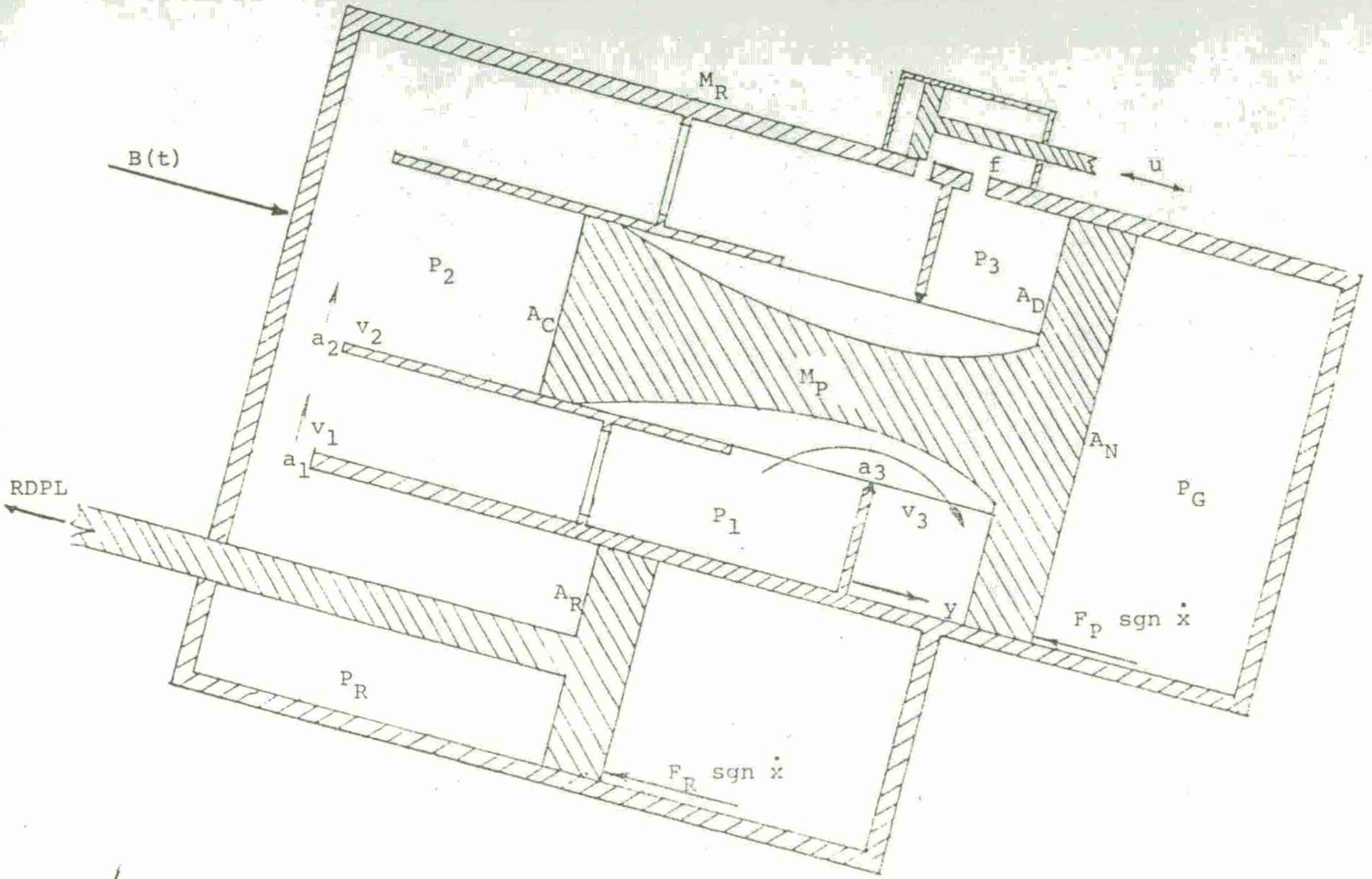

Figure 8. BLOCK DIAGRAM OF MODIFIED RECOIL MECHANISM

$$C_q = A_R T_1 + \frac{A_R}{A_N}(A_C T_2 + A_D T_3)$$

and

$$T_3 = \left(\frac{\rho}{2}\right)\left(\frac{A_0}{C_3}\frac{A_R}{A_N(A_3+u)}\right)^2 \qquad (16)$$

The modified form of the model is

$$m\ddot{x} + [a+f(x)+u(x,\dot{x})]\,\dot{x}^2 \operatorname{sgn}\dot{x} + k(1-a_0 x)^{-R} + F\operatorname{sgn}\dot{x} = W + B(t)$$

The task of finding optimal values g_1 and g_2 of the feedback gains is formulated as follows.

Find optimal values of g_1 and g_2 such that an objective function $J(g_1, g_2)$ is minimized subject to the following constraints. The system follows the model

1) $$m_q\ddot{x} + C_q\dot{x}^2\operatorname{sgn}\dot{x} + F_q\operatorname{sgn}\dot{x} + A_R P_0\left(1-\frac{A_R}{V_0}x\right)^{-R} = W_q + B(t)$$

where

$$C_q = A_R T_1 + \frac{A_R}{A_N}(A_C T_2 + A_D T_3)$$

$$T_3 = \left(\frac{\rho}{2}\right)\left(\frac{A_0}{C_3}\frac{A_R}{A_N}\right)^2 \frac{1}{(A_3 + g_1 x + g_2 \dot{x})^2}$$

2) X_{max}, the maximum recoil length

$\leq X_m$, the available recoil length

3) There is no cavitation in chamber 3, i.e.,

$P_3(t) \geq P_{3\,min}$

4) The maximum servovalve area $u = g_1 x + g_2 \dot{x}$

$U_{max} \leq U_m$

3.2 Development of an Objective Function

The basic performance criterion is that the actual rod pull trajectory should follow as closely as possible the desired control trajectory for every zone. So let the control trajectory be RDPLD(t)

Then,

$$J(g_1, g_2) = \int_0^T [RDPLD(t) - RDPL(t)]^2 \, dt$$

will represent the integrated error or least square error criterion. To be able to use unconstrained optimization techniques, penalty functions can be added to take care of constraints and hence the penalty functions are

$$J_2 = \int_0^T w_2 (P_3(t) - P_{3\ min})^2 \, dt$$

$$J_3 = \int_0^T w_3 (U(t) - U_m)^2 \, dt$$

$$J_4 = \int_0^T w_4 \, (x - x_m)^2 \, dt$$

where $w_2 = 0 \quad P_3(t) > P_{3min}$

$w_3 = 0 \quad U(t) < U_m$

$w_4 = 0 \quad x < x_m$

So the composite objective function is

$$J(g_1,g_2) = \int_0^T \{w_1 (RDPLD(t) - RDPL(t))^2 + w_2(P_3(t) - P_{3\ min})^2 + w_3(U(t) - U_m)^2 + w_4(x-x_m)^2 \}\ dt$$

By choosing w_2, w_3, w_4 large postive numbers, the constraint violations can be avoided.

The VA10A optimization routine availible on UNIVAC 1110 at UWMACC which uses Davidon - Fletcher - Powell (Appendix III) method was used to find optimal values of g_1, g_2 for zone 7 and results are shown in figure 9, 10. The control trajectory was chosen arbitrarily. Figure 9 is with no feedback and 10 is with optimal feedback gains of g_1 = .2742E-3 and g_2 = .354E-7. The actual trajectory follows the desired trajectory in Fig. 10 more closely than in Fig. 9.

The procedure was repeated for other zones with arbitrary control trajectory. The optimization procedure is very sensitive to the definition of the control trajectory and thus redefinition of the objective function without the control trajectory is necessary. The main objective can be reiterated as the minimization of rod pull and a flat trajectory to avoid sudden or sharp changes which induce fatigue failure. The first derivative represents the smoothness or flatness of the trajectory to some extent and hence, a penalty for large first derivatives can be added to the objective function.

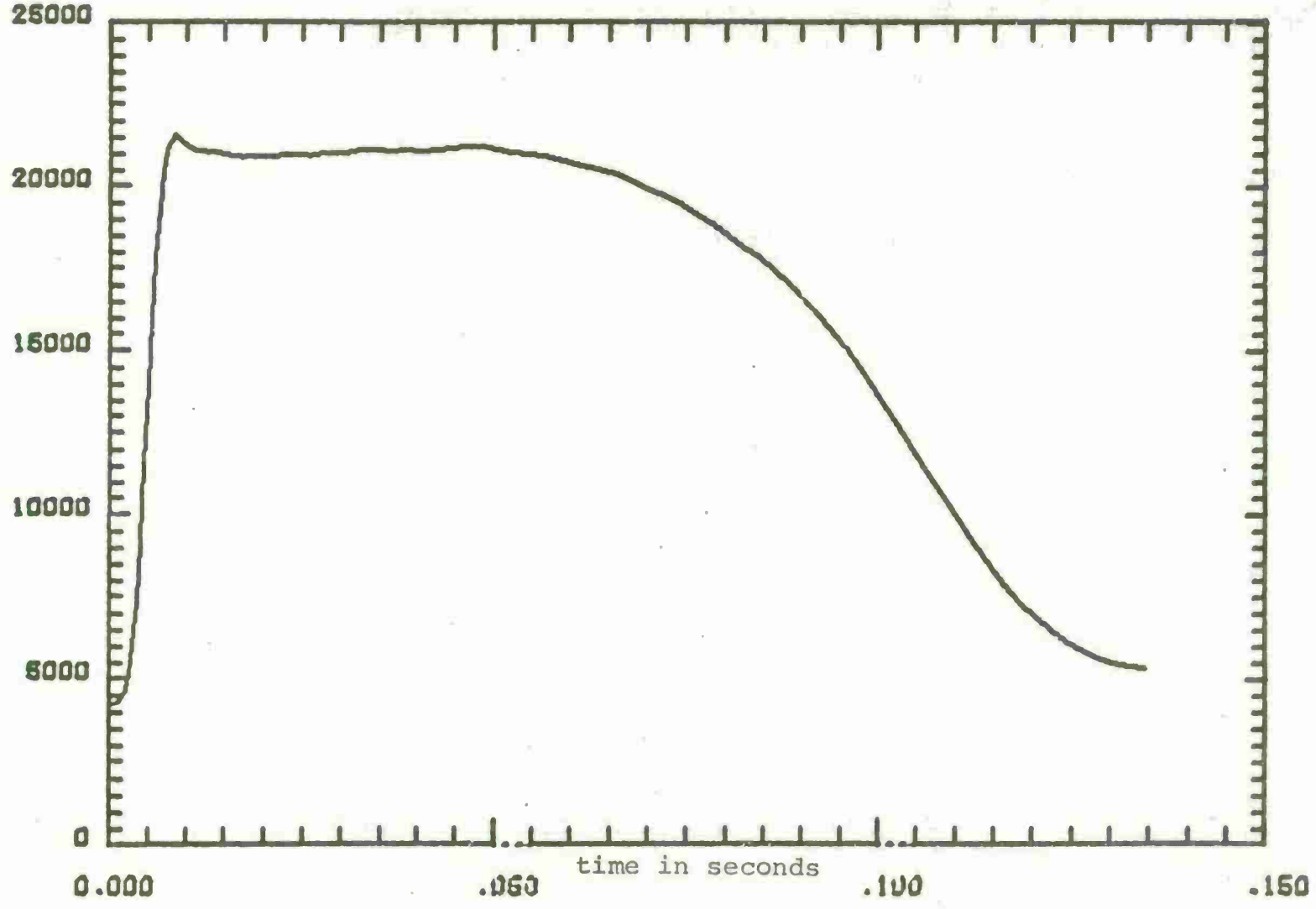

Figure 9 Rod Pull for Zone 7 with No Feedback

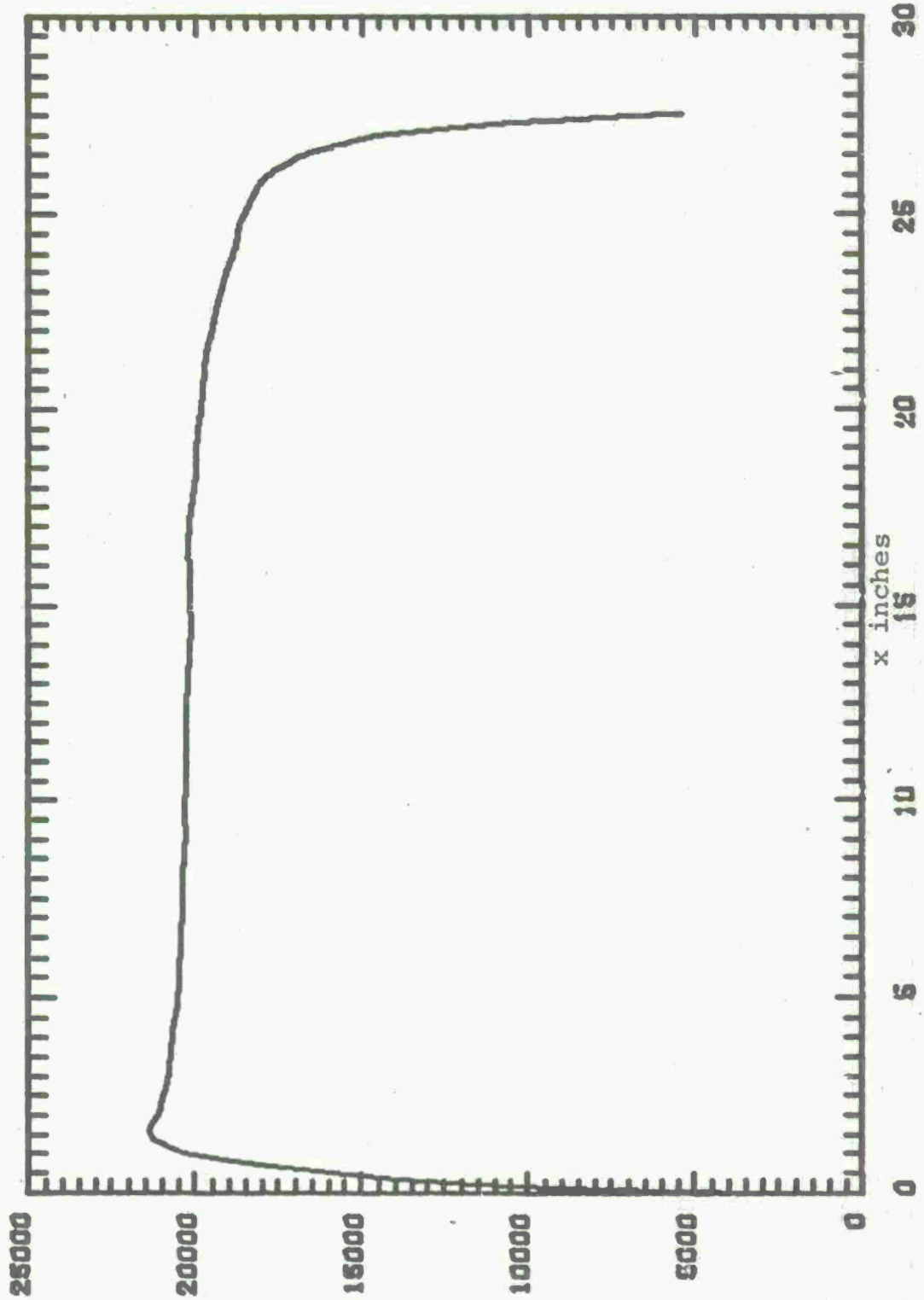

Figure 10 Rod Pull for Zone 7 With Linear Feedback i.

The new composite objective function can be written in five parts as

$$J_1 = \int_0^T (RDPL(t) - C)^2 \, dt$$

where C is a constant = 4200.

Penalty for non-smoothness

$$J_2 = \int_0^T \{\frac{\partial}{dt} RDPL(t) \}^2 \, dt$$

Penalty for constraint violation for cavitation

$$J_3 = \int_0^T (P_3(t) - P_{3\ min})^2 \, dt$$

Penalty for maximum servo-valve area constraint

$$J_4 = \int_0^T (U(t) - U_m)^2 \, dt$$

Penalty for maximum recoil length constraint

$$J_5 = \int_0^T (X - X_m)^2 \, dt$$

The composite objective function being

$$J = w_1J_1 + w_2J_2 + w_3J_3 + w_4J_4 + w_5J_5$$

with $w_3 = 0$ if $P_3(t) > P_{3\ min}$

$w_4 = 0$ if $U(t) \leq U_m$

$w_5 = 0$ if $X < X_m$

The weighting factors w_1 and w_2 provide a trade off between the minimum error and flatness of the rod pull trajectory. Large w_1 with respect to w_2 will result in sharp trajectory with a peak in initial stage of recoil.

Large w_2 with respect to w_1 will result in a sharp peak at a later stage in recoil and also possibly will result in cavitation at variable area orifice 3. By choosing w_1 and w_2 in between these extremes, a satisfactory shape of the trajectory can be achieved.

The weighting factors w_3, w_4, and w_5 emphasize or de-emphasize the penalty functions for constraint violations. If any constraint is violated, the corresponding weighting factor can be increased so as to force the optimization algorithm to choose a feasible solution.

3.3 Results for M-37 Recoil Mechanism

The linear state feedback control system and optimization procedure discussed in Sections 3.1 and 3.2 was applied to M-37 recoil mechanism. M-37 was designed for a firing charge zone 7. The design data and breech forces for zones 1, 5, 6, 7, and 8 are tabulated in Appendix III and was provided by the Ware Simulation Division at Rock Island Arsenal. The breech forces used are from simulated breech forces. The breech force for zone 8 was arrived at by multiplying breech force for zone 7 by 1.2 due to unavailability of data.

The feedback gains for zones 5, 6, 7, and 8 and other parameters are presented in Table 1. The rod pull characteristics are plotted in Figures 11 through 20 with no feedback and with optimal feedback.

Figures 11 and 13 portray the time history of the rod pull for no feedback and optimum linear feedback control for zone 8. Zone 8 was arrived at by multiplying zone 7 breech force by 1.2. Though the trajectory for no feedback looks very satisfactory, the Figure 12 which plots the pressure $P_3(t)$ reveals that there is cavitation and hence the model is no longer valid. Figure 13 shows trajectory not very flat but there is no cavitation as shown in Fig. 14. This is achieved through optimization with penalty for cavitation. With Random

Table 1 Results of Optimum Feedback for Zones 5, 6, 7 and 8

Zone	Gains g_1	Gains g_2	Recoil Length (in)	Recoil Time (sec)	Rod Pull Maximum (lbs)	Servo Value Area Maximum (in^2)
8	0	0	27	.126	25,200 Cavitation	0
8	.81E-4	.884E-5	27.6	.12	25,800 No Cavitation	.005
7	0	0	27	.13	Max^m 21,500 Flat 21,000	0
7	.1803E-3	.532E-5	27.6	.13	Max^m 21,000 Flat 20,500	.0054
6	0	0	25.8	.17	14,700	0
6	.17E-3	.376E-4	27.2673	.158	12,900	.0134
5	0	0	24	.19	11,360	0
5	.6591E-3	.1E-3	28.1647	.194	Max^m 8,800 Flat 8,500	.032

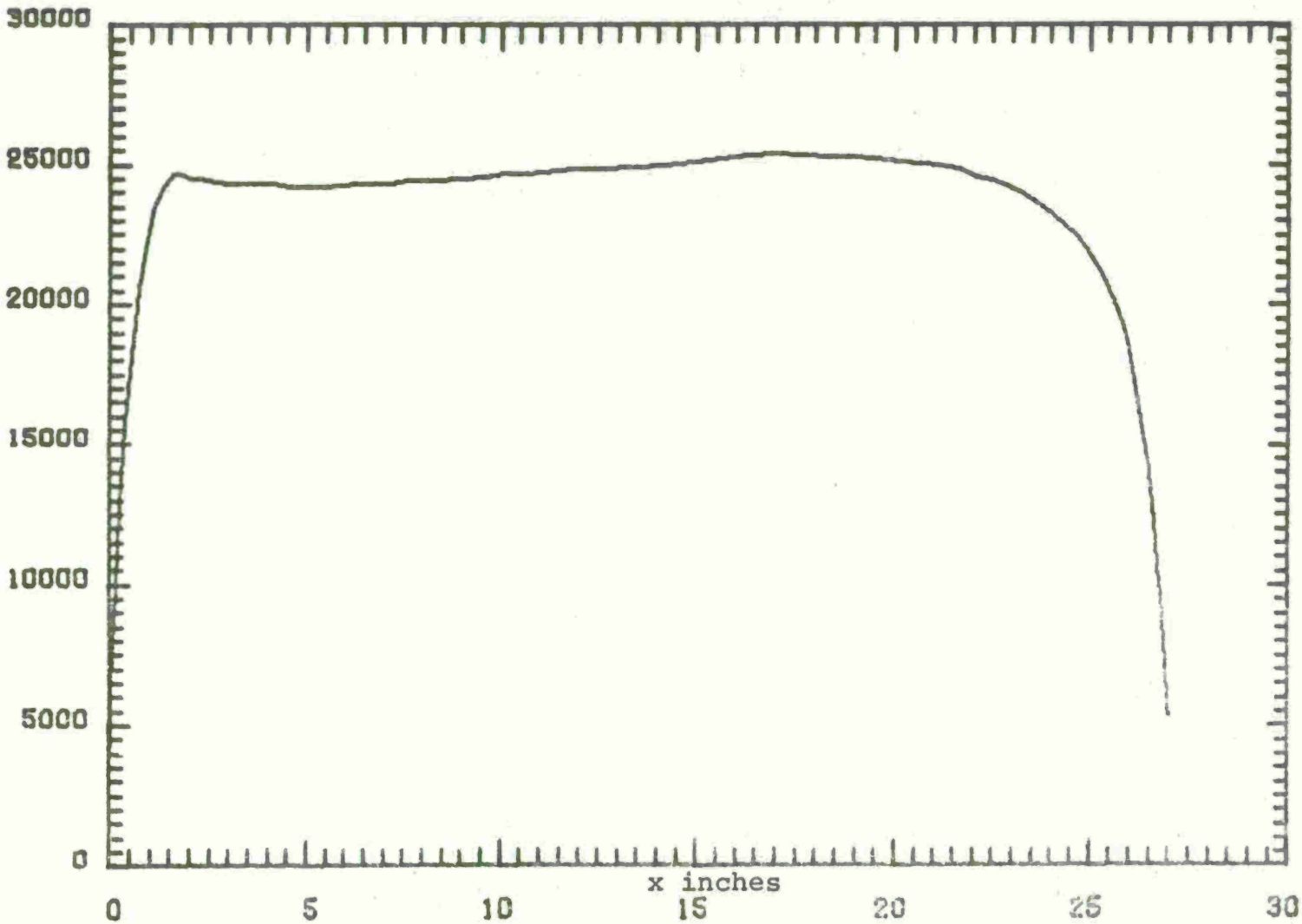

Figure 11 Rod Pull for Zone 8 with No Feedback

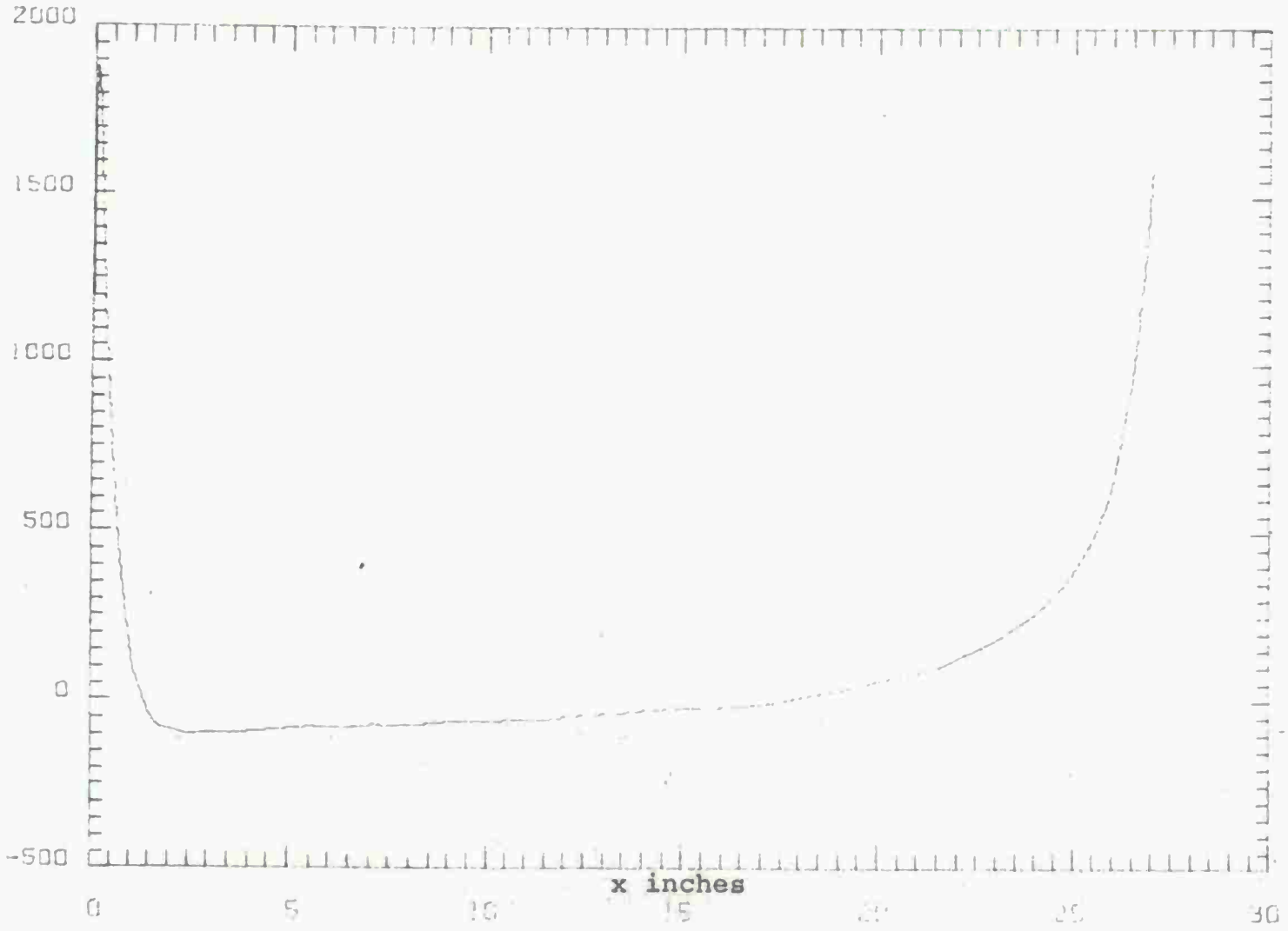

Figure 12 Cavitation Pressure for Zone 8 with No Feedback

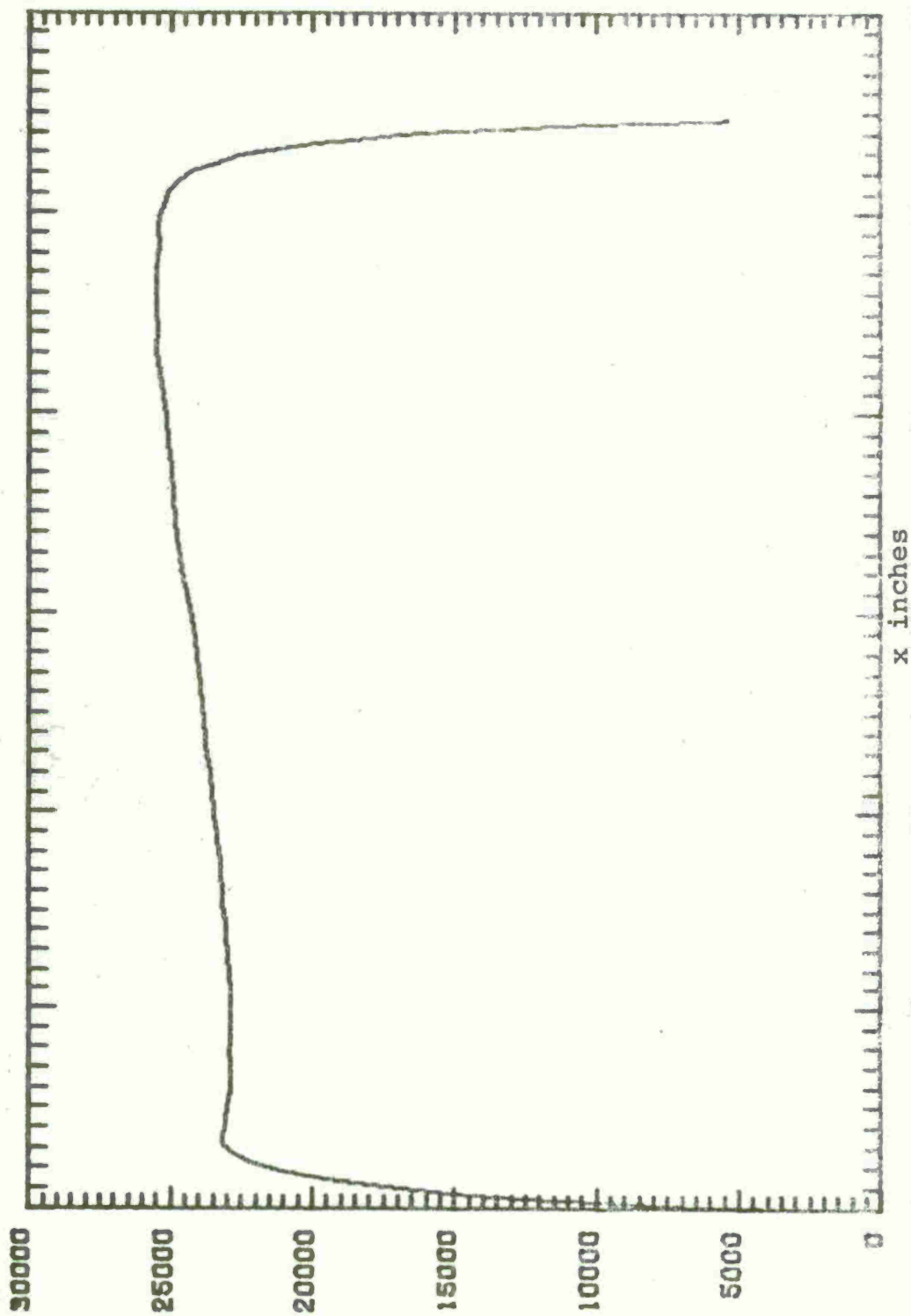

Figure 13 Rod Pull for Zone 8 with Feedback

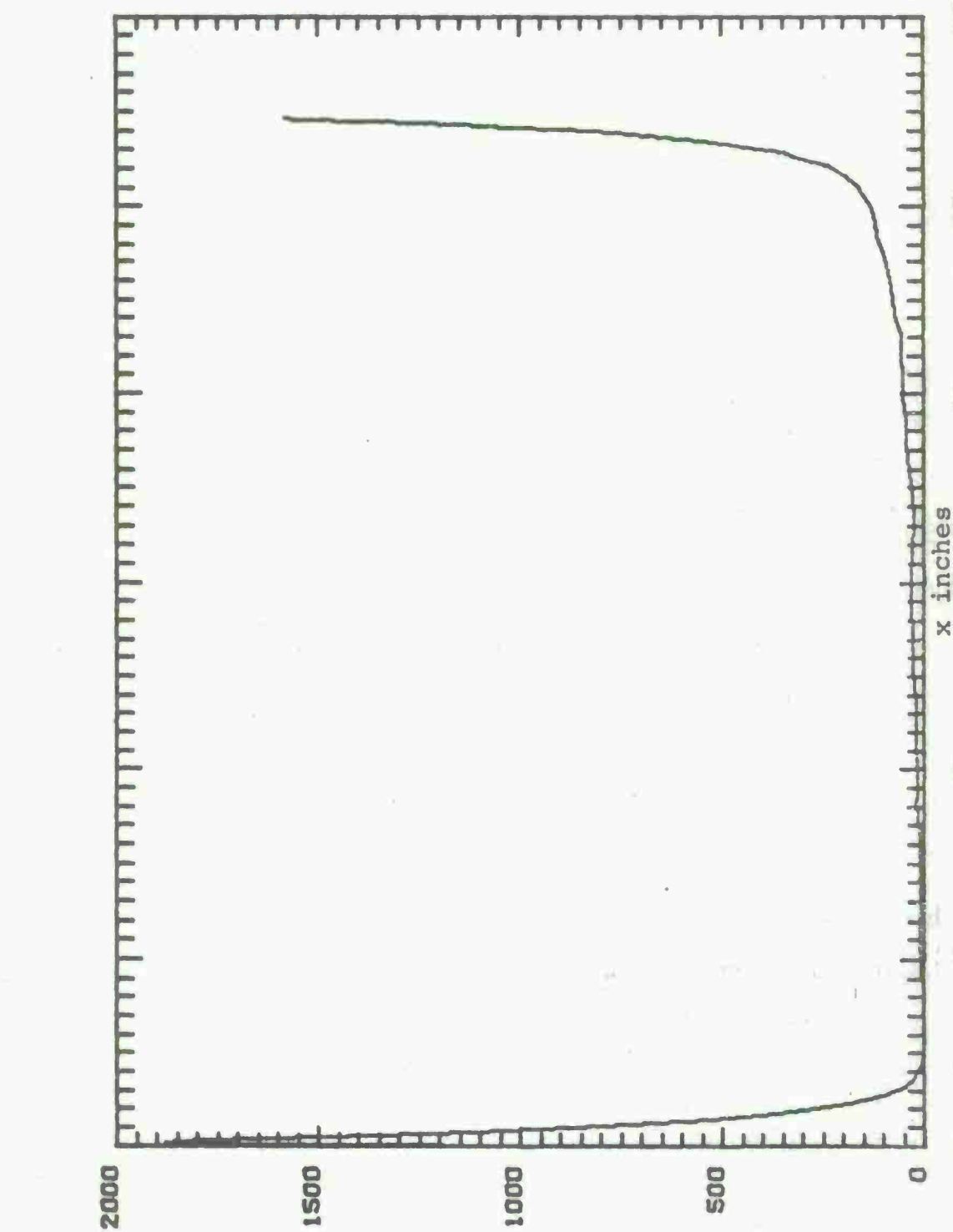

Figure 14 Cavitation Pressure for Zone 8 with Feedback

Search technique $P_{3\ min}$ was increased up to 20 psi. With reasonable $P_{3\ min}$, cavitation can completely be eliminated.

Figures 15 and 16 are rod pull trajectories for zone 7 with no feedback and with optimal feedback. The improvement is not significant. The improvement was significant as shown in Figures 9 and 10 even for zone 7 with the first objective function. The relative improvement in peak force is about 2.5% and recoil length is longer by 0.6 inches. There is no change in the total recoil time of .13 seconds.

The rod pull trajectory for zone 6 with no feedback is a more triangular with maximum rod pull of 14,700 lbs. (Figure 17). The optimal feedback control law results in a very flat trajectory with maximum force of 12,900 which is a significant reduction of about 12% (Figure 18). The recoil length is increased from 25.8 inches to 27.27 inches but recoil time is reduced from .17 seconds to .158 seconds.

The rod pull trajectory for zone 5 with no feedback is a sharp triangular one with peak of 11,360 lbs. (Figure 19). The optimal feedback control law reduces this force to 8500 lbs with a flat and trapezoidal trajectory. The recoil length and time are both increased. The percentage reduction in recoil force is 25%.

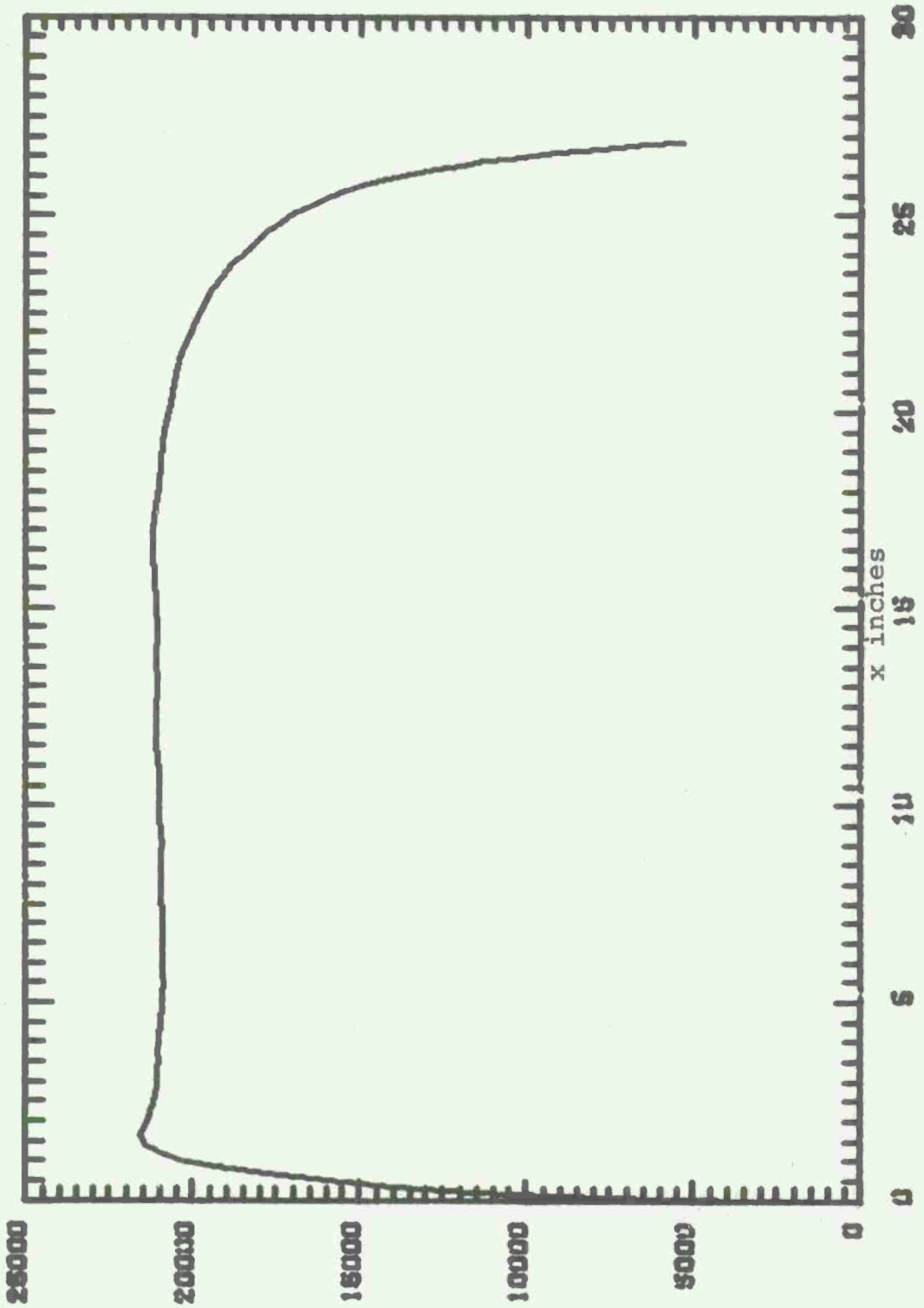

Figure 15 Rod Pull for Zone 7 With No Feedback

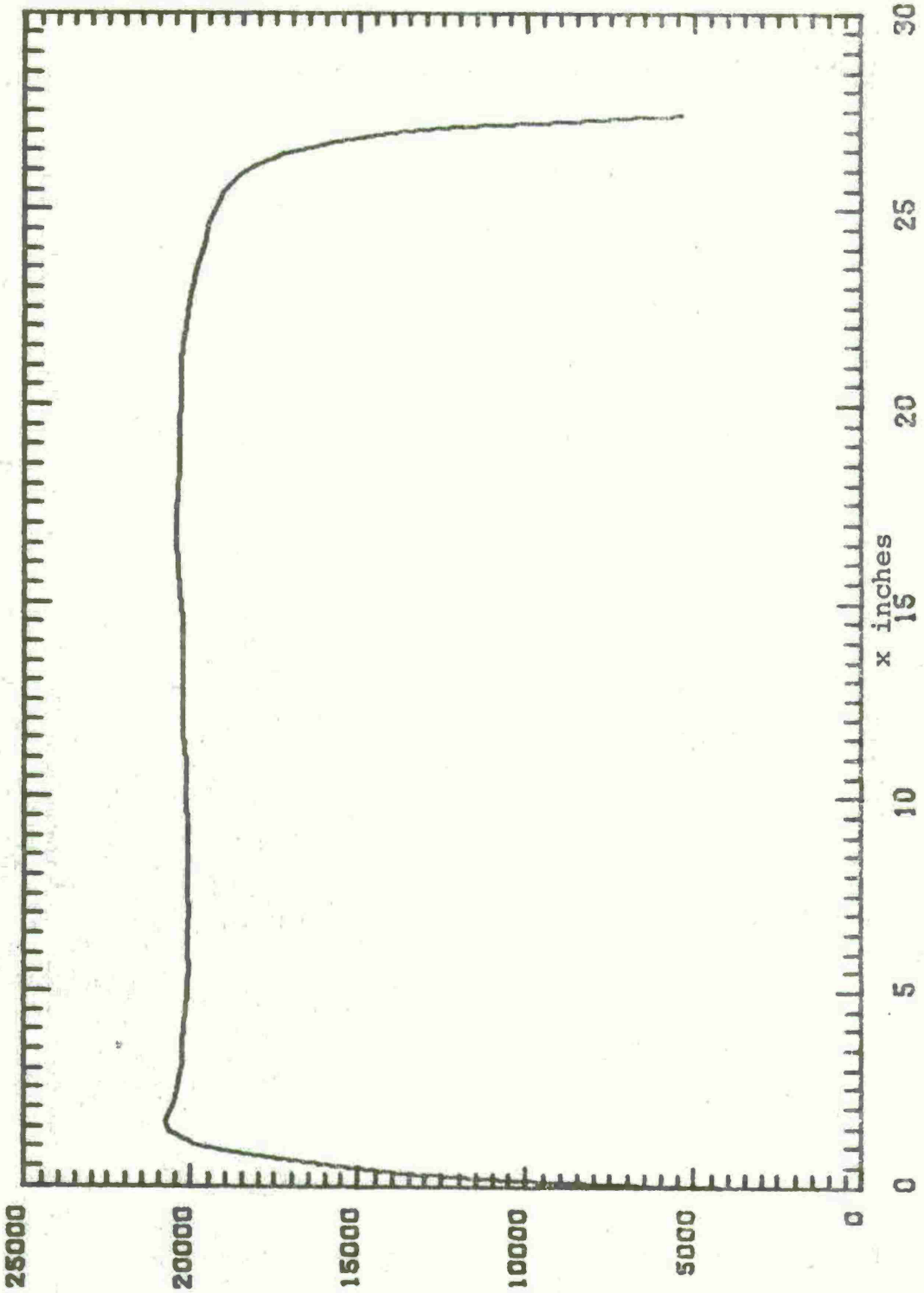

Figure 16 Rod Pull for Zone 7 with Feedback

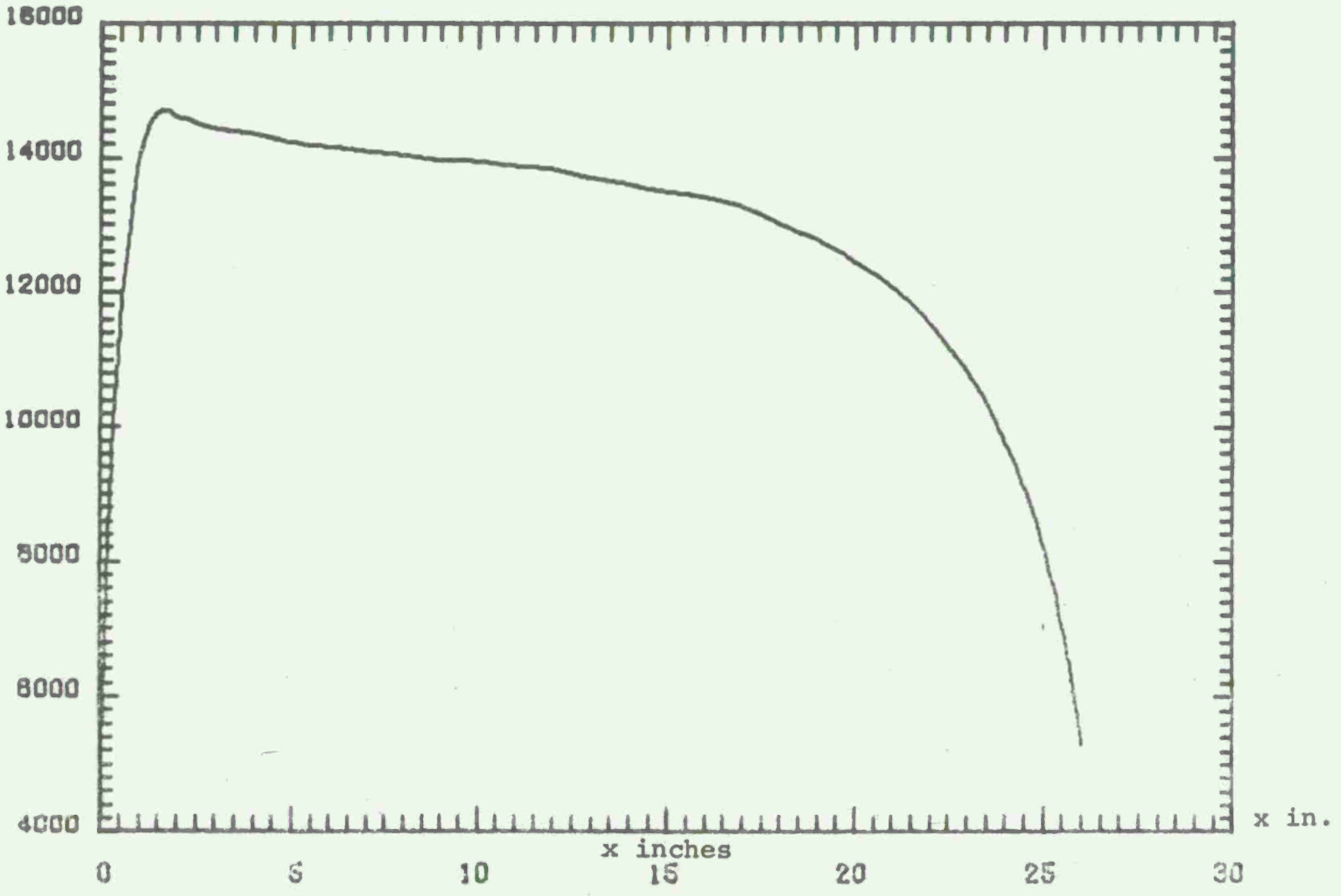

Figure 17 Rod Pull for Zone 6 with No Feedback

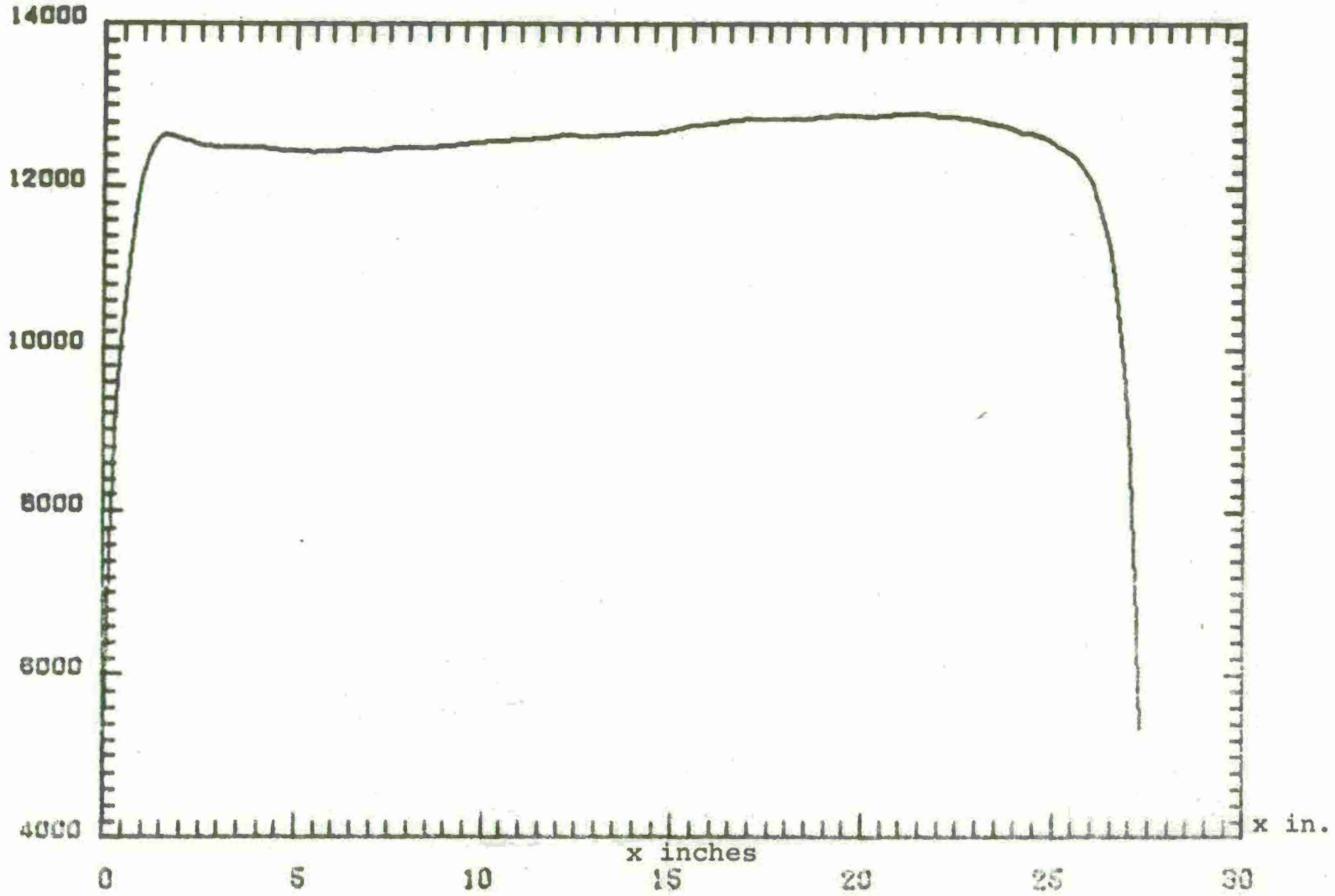

Figure 18 Rod Pull for Zone 6 with Feedback

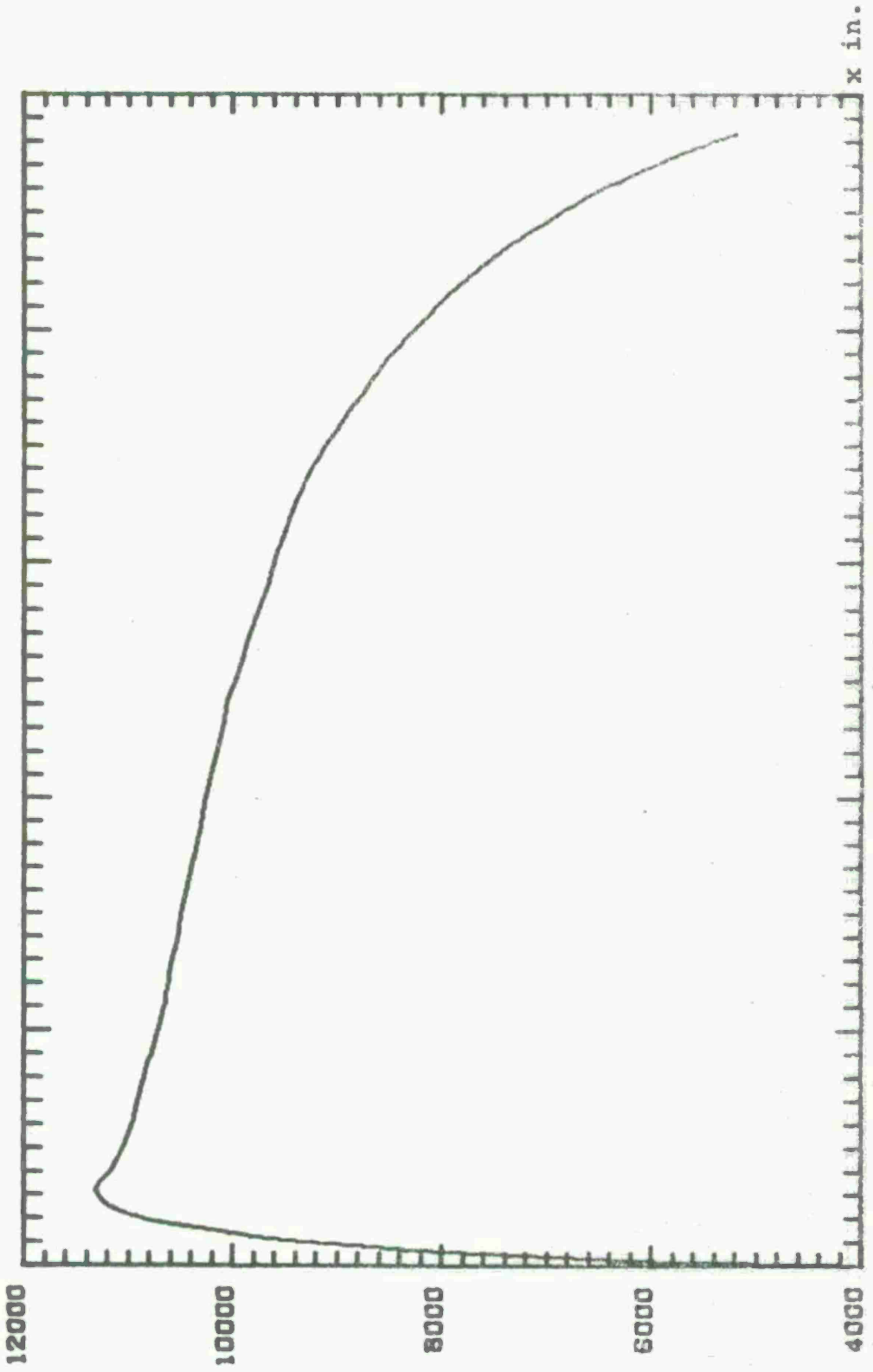

Figure 19 Rod Pull for Zone 5 with No Feedback

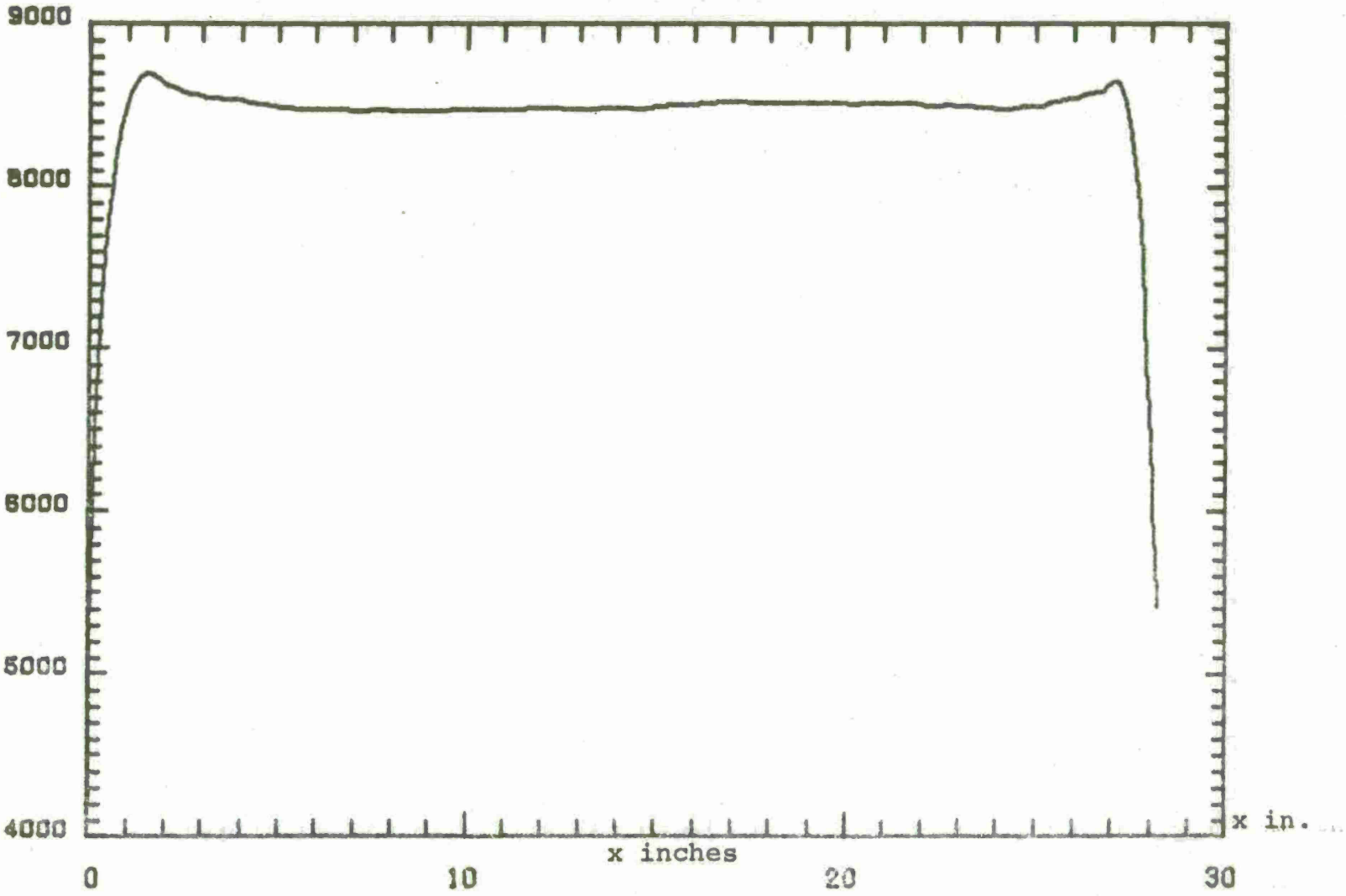

Figure 20 Rod Pull for Zone 5 with Feedback

3.4 Tachometer Feedback

To investigate different control strategies, only velocity feedback of the form $u = g_1\dot{x}$ was studied. In general, it worked very well for lower zones 6, 5 and 1 but failed to improve the trajectories for zone 7 and made it worse for zone 8. The optimum feedback gain was arrived at by trial and error.

Trajectory for zone 7 with tachometer feedback gain $g_1 = .006E-3$ (Fig. 21) is not much of an improvement over one without feedback (Fig.15). Fig. 22 for zone 6 with $g_1 = .025E-3$ shows a substantial improvement over Fig. 17, the maximum force being 13,200 lbs.; though it is not better than linear state feedback (Fig.18). Fig. 23 for zone 5 with $g_1 = .07E-3$ is trapezoidal and significant reduction in maximum rod pull to 9,400 lbs., but is not better than linear state feedback of Fig. 20. Trajectory for zone 1 with $g_1 = .35E-3$ (Fig. 24) is also very good with reduction to 5,350 lbs. over Fig. 25 (24%).

Non-linear feedback control laws of the form

$$U = g_1x + g_2\dot{x} + g_3x^2 + g_4\dot{x}^2$$

were investigated for zone 7. The trajectory obtained were with no improvement and sometimes were worse than those with no feedback.

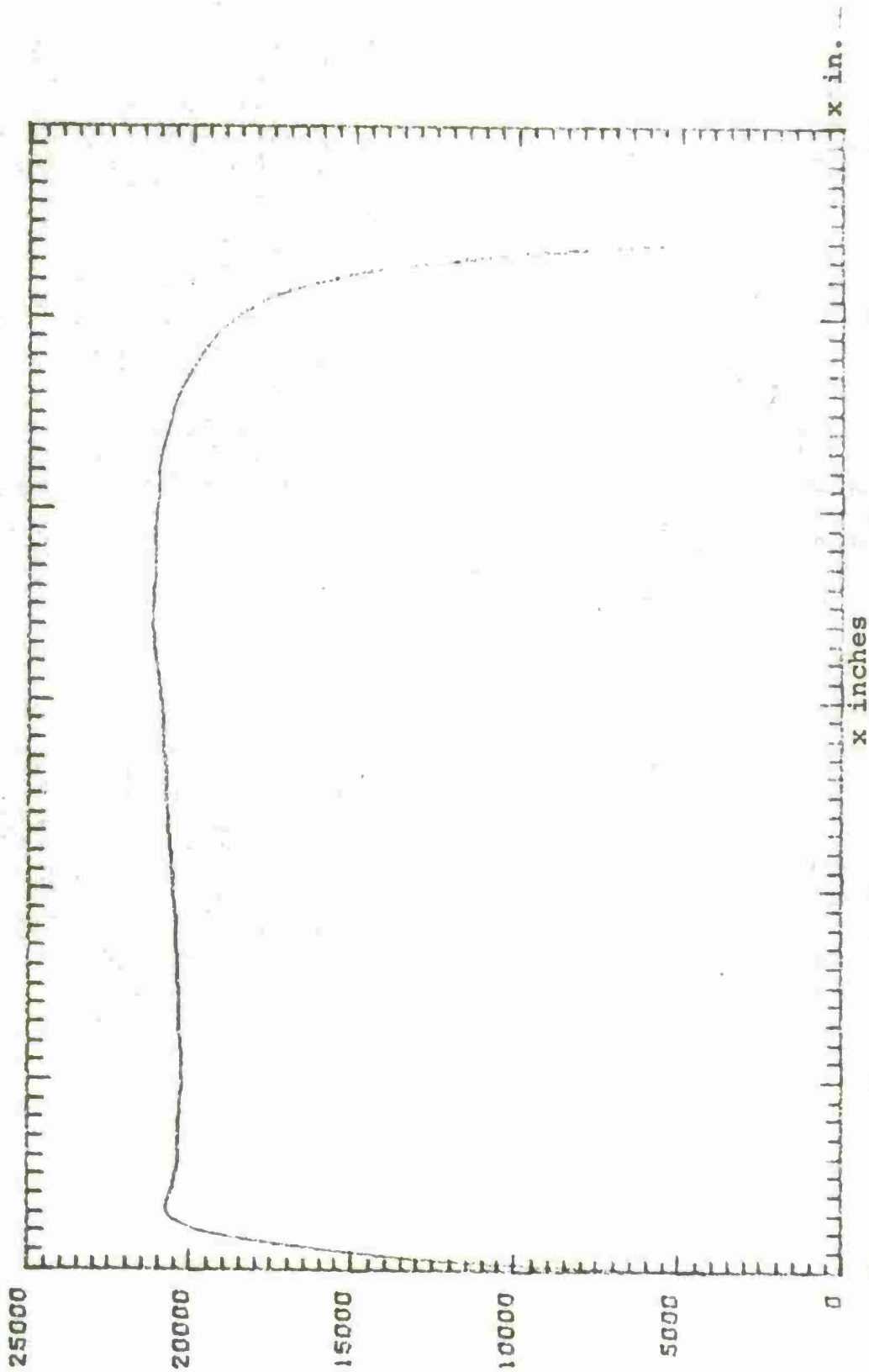

Figure 21 Rod Pull for Zone 7 with Velocity Feedback

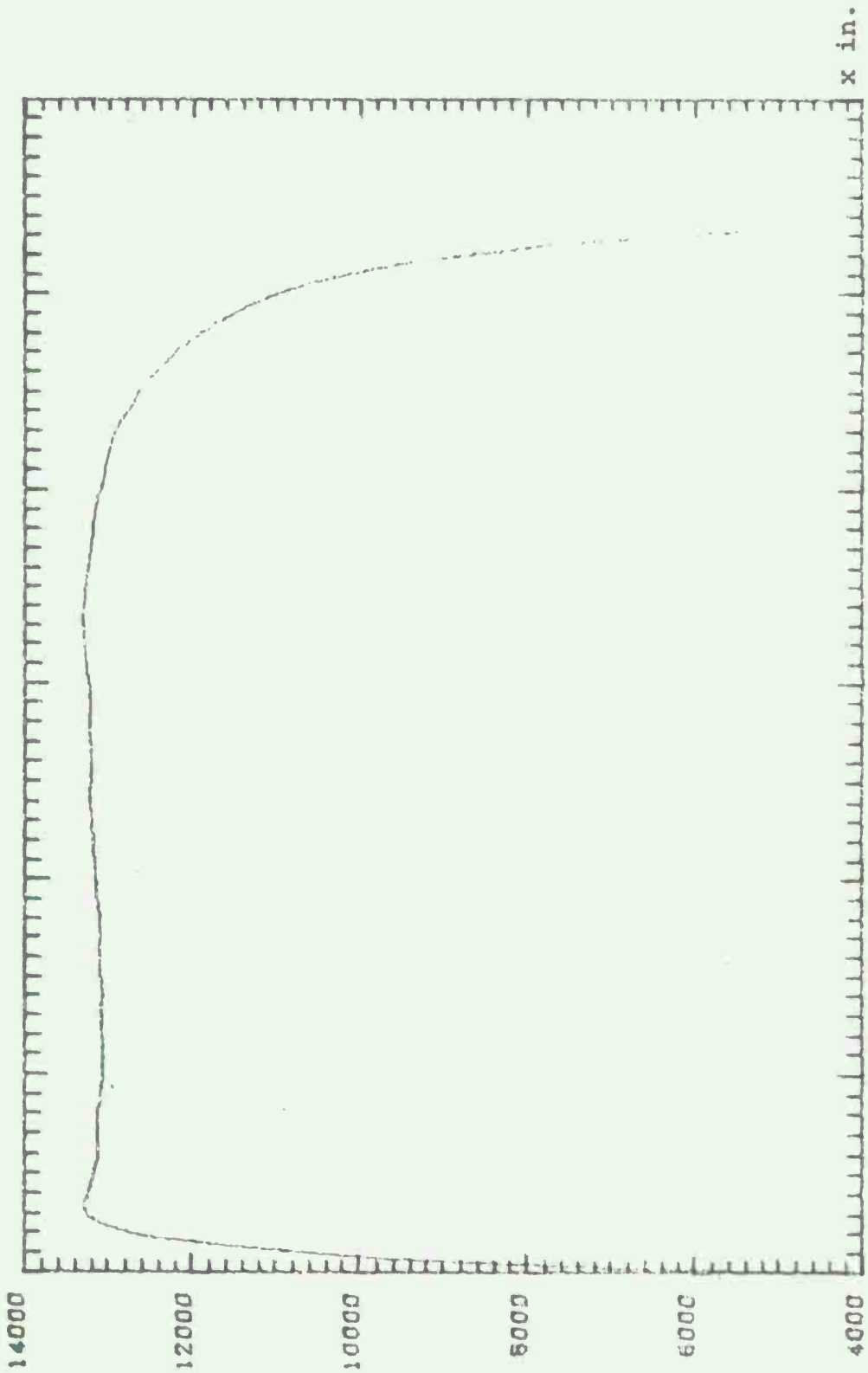

Figure 22 Rod Pull for Zone 6 with Velocity Feedback

Figure 23 Rod Pull for Zone 5 with Velocity Feedback

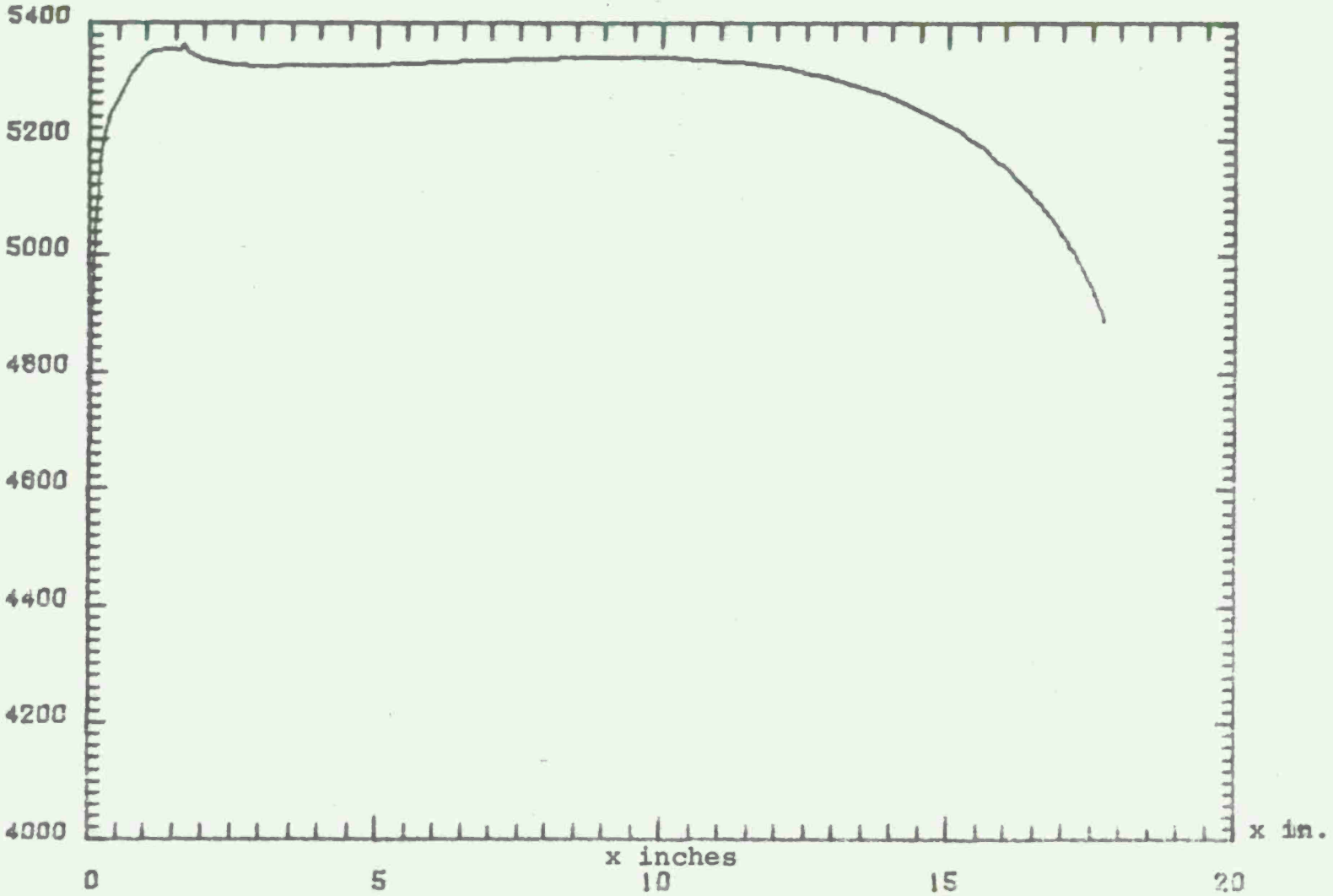

Figure 24 Rod Pull for Zone 1 with Velocity Feedback

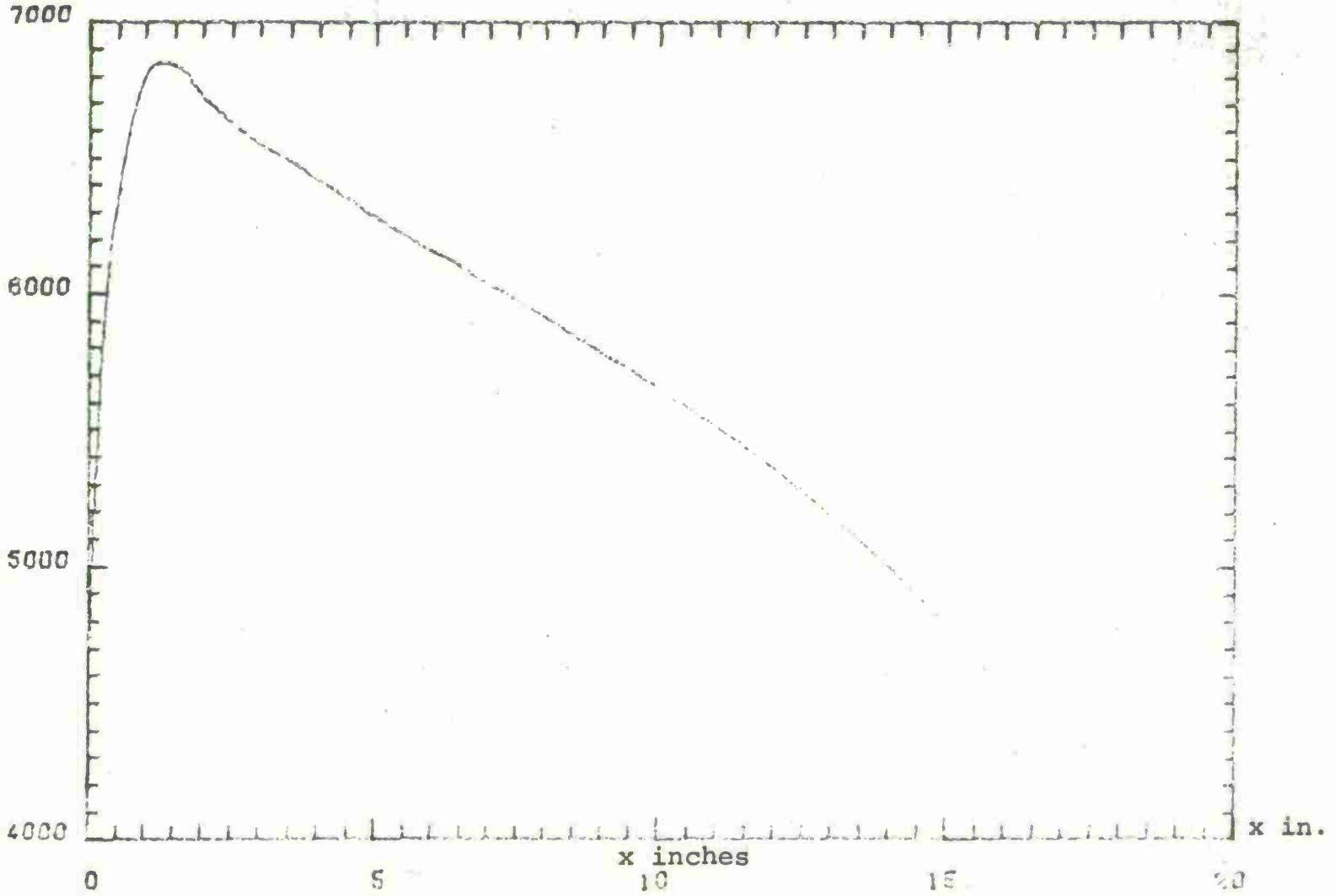

Figure 25 Rod Pull for Zone 1 with No Feedback

CONCLUSIONS

A mathematical model for a conventional hydropneumatic recoil mechanism was developed and simulated on a digital computer by method of Phase-Plane-Delta. A linear state feedback control system was proposed which can be implemented by retrofitting the present designs with a servo-valve to operate in tandem with the variable area groove in the floating piston.

An objective function with direct relation to performance and physical constraints of the system was developed. Davidon-Fletcher-Powell nonlinear optimization algorithm was chosen to optimize this objective function. The procedure was applied to M-37. recoil mechanism with reduction in peak recoil forces from 25 to 2.5% for lower zones and cavitation was avoided for zone 8. Tachometer feedback was shown to be effective for low zones.

The concept of feedback control system coupled with optimization procedure to design recoil mechanisms was demonstrated to be an efficient and very effective tool. The flexibility of feedback control is added retaining robustness of design.

The techniques of feedback control and optimization procedures are recommended for design of counter recoil and other design problems in recoil mechanism.

REFERENCES

1. Seireg, Ali, Mechanical Systems Analysis, International Textbook Company, 1969.

2. Gottfried, Byron S. and Weisman, Joel, Introduction to Optimization, Prentice-Hall Inc., Englewood Cliffs, New Jersey, 1973.

3. Walsh, G.R., Methods of Optimization, John Wiley & Sons, New York, 1975.

4. Bellman, Richard, Mathematical Optimization Techniques, University of California Press, Berkley, 1963.

5. Adby, P.R. and Dempster, M.A.H., Introduction to Optimization Methods, Chapman and Hall, London, 1974.

6. Box, M.J., "A New Method of Constrained Optimization and a Comparison With Other Methods," The Computer Journal, 8, pp. 42-52, 1975.

7. Box, M.J., "A Comparison of Several Current Optimization Methods and the Use of Transformations in Constrained Optimization," The Computer Journal, 9, pp. 67-77, 1966.

8. Nerdahl, M.C. and Frantz, J.W., "Development of a Mathematical Model for Designing Functional Controls of a Soft-Recoil Mechanism," Army Weapons Command, Rock Island, Illinois, AD 713565.

9. Nerdahl, M.C. and Frantz, J.W., "Engineering Analysis, Recoil Mechanisms, XM45 Design of Control Grooves and Prediction of System Motion," Army Weapons Command, Rock Island, Ill. Research and Engineering Directorate, AD-876 531L, October 1970.

10. Frantz, J.W. and Nerdahl, M.C., "Mathematical Models for Engineering Analysis and Design of Howitzer, Medium, Towed, 155 mm, XM198," Artillery Systems Laboratory, Research and Engineering Directorate, U.S. Army Weapons Command, Rock Island, Ill., AD-876775L, October 1970.

Appendix I

Phase-plane-delta simulation of non-linear systems

Phase-plane-delta method is an efficient and fast simulation method for non-linear second order differential equations. A generalized phase plane method is also suitable for higher order non-linear differential models; for details see "Mechanical Systems Analysis" by A. Seireg [1]. The procedure is discussed below for second order equation reproduced with some variation from Prof. Seireg's book.

Consider a linear homogeneous second order differential equation

$$\ddot{x} + w_n^2 x = 0 \qquad (1)$$

The solution to this equation being

$$x = A \sin (w_n t + \phi) \qquad (2)$$

$$\dot{x} = A w_n \cos (w_n t + \phi) \qquad (3)$$

From equation 2 and 3, it can be seen that

$$x^2 + \left(\frac{\dot{x}}{w_n}\right)^2 = A^2$$

which represents a circle in the x versus $\frac{\dot{x}}{w_n}$ plane. This type of plot is known as the phase plane and is a very powerful and useful tool in the analysis of dynamic problems. It could be seen from Fig.26 that the horizontal projection of the motion on a time scale will give the velocity curve plotted to a scale w_n. The

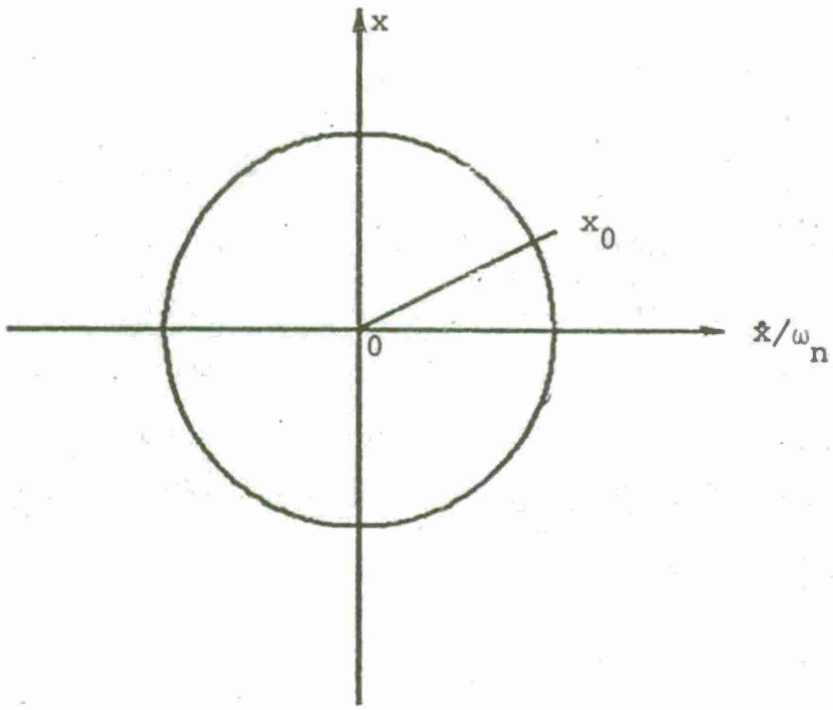

Figure 26 Phase Plane Method

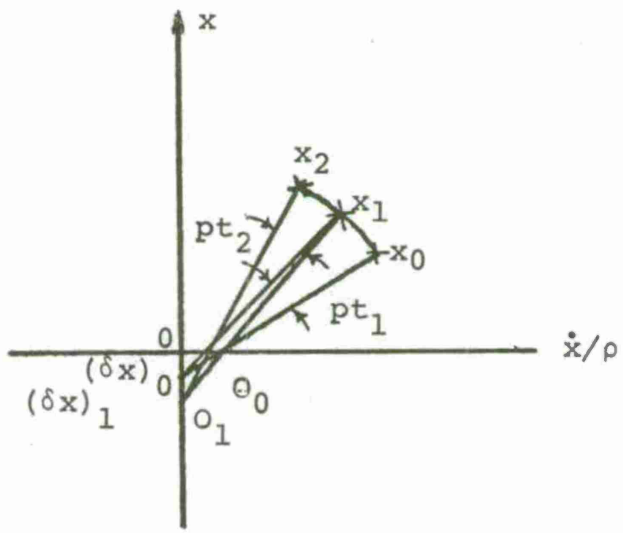

Figure 27 Phase Plane Delta Method

starting point X_0 on the circle is defined by initial conditions at t = 0, say $x = x_0$ and $\dot{x} = \dot{x}_0$; the amplitude of motion being

$$A = \sqrt{x_0^2 + (\dot{x}_0/w_n)^2}$$

The complete procedure is detailed step by step as follows

1) Calculate the natural frequency w_n of the system
2) Plot the two perpendicular axes representing x and $(\dot{x}/w_n)$ respectively. These two axes represent the phase plane.
3) The origin O of the phase plane represents the equilibrium condition of the system.
4) Knowing the initial conditions of the motion in terms of initial displacement and velocity, a point X_0 can be plotted in the phase plane.
5) The free vibration of the system is represented by a circle. The center of the circle is the equilibrium point O. The radius of the circle is the distance OX_0 joining the origin to the initial point X_0.
6) The conditions of motion at any time t_1 are represented by the coordinates of the point X_1 on the circle at a radial angle $w_n t_1$ from X_0 in the counterclockwise direction.

7) The projection of the phase-plane plot on a time scale in the direction of x, $(\frac{\dot{x}}{w_n})$ gives the displacement and velocity functions respectively.

8) All information concerning the time history of the motion can be obtained fron the phase-plane plot.

This scheme can be implemented on a digital computer

The phase-plane-delta method

The phase plane method previously discussed is used to study free vibrations of a linear system. With a slight modification, phase-plane method can be used for forced non-linear vibration problems as follows.

Let the system be

$$m\ddot{x} + k\, f(x,\dot{x},t) - F(t) = 0 \qquad (4)$$

Rewriting the equation

$$\ddot{x} + \frac{k}{m}[\dot{x} + f(x,\dot{x},t) - x - F(t)/k\ ] = 0$$

or

$$\ddot{x} + p^2\ [x + \delta x] = 0 \qquad (5)$$

where $\delta x = [f(x,\dot{x},t) - x - F(t)/k\ ]$ & $p = \sqrt{k/m}$ and is a known function of x, $\dot{x}$, t, F(t). Equation 5 takes the same form as equation 1 where p^2 takes the place of w_n^2 and x has to be continually modified by an amount δx which is a function x, $\dot{x}$, t, and F(t).

Therefore, at any instant of time the nonlinear equation can be represented in the phase-plane as a free vibration of a linear system with a continually changing datum.

The procedure is outlined step by step as follows.

1) Write the equation in the form

$$\ddot{x} + p^2 (x + \delta x) = 0$$

where p^2 is a constant.

2) Express δx as a function x, $\dot{x}$, t, $F(t)$.

3) Plot the phase plane axes to represent x, $(\dot{x}/p)$ Fig. 27.

4) Knowing initial conditions x_0, $\dot{x}_0$, a point X_0 can be plotted in the phase plane.

5) The value of $(\delta x)_0$ is also calculated for the initial condition at time $t = t_0$.

6) The center O_0 of the instantaneous linear vibration at the initial phase of the motion is therefore located on the x-axis at a distance $(\delta x)_0$ from the origin. When δ is positive, the distance is taken on the negative x-axis and vice-versa.

7) The instantaneous free vibration at the initial phase of the motion can be represented by a small arc of a circle with center O_0 and radius O_0X_0 in the counter-clockwise direction.

8) A new condition X_1 is reached after a small increment of time t_1 where the displacement x_1 and the velocity is $\dot{x}_1$.

9) The value of $(\delta x)_1$ corresponding to this new condition can be calculated, and a new center of oscillation O_1 is determined.

10) The new condition X_2 corresponding to an additional increment of time t_2 can be obtained from the arc of a circle with center O_1, having a radius O_1X_1 and subtending an angle pt_2 in the counterclockwise direction.

11) This procedure is then repeated until the time required is reached.

12) It should be noted here that the accuracy of this procedure depends on the magnitude of the angular displacement pt. Better accuracy can be attained also by iteration. This means that after X_1 is determined, a value of δx is calculated which corresponds to a point midway between X_0 and X_1. Using this new value of δx, a better approximation for the new position X_1 after a small increment of time t_1 can be obtained. This procedure can be repeated until a desired accuracy is achieved.

13) This procedure is suitable for programming on a high-speed digital computer.

APPENDIX II

ALGORITHMS FOR OPTIMIZATION OF NON-LINEAR FUNCTIONS

Three algorithms for non-linear optimization are discussed:

1) Davidon-Fletcher-Powell unconstrained optimization with cubic interpolation.
2) Davidon-Fletcher-Powell unconstrained optimization with linear search by golden section.
3) Constrained optimization by Random search.

A short introduction to gradient methods of optimization is presented.

The problem of non-linear optimization can be stated as

Find a vector $\underset{\sim}{x}$ of parameters to minimize

$J(x)$, an objective function subject to certain constraint of type

$$C_i(x) \leq , = \text{or} \geq b_i$$

We can express $J(x)$ in Taylor series expansion as

$$J(x+\Delta x) = J(x) + \Delta x' g + \frac{1}{2} \Delta x' G \Delta x + \ldots \qquad (1)$$

where Δx is a vector of increment in $\underset{\sim}{x}$

g is the gradient vector

G is the Hessian Matrix of second order partial derivatives

The first order approximation is

$$J(x+\Delta x) = J(x) + \Delta x' g$$

The reduction in the function J(x) for moving to x+Δx is Δx'g and is maximum if we move in the negative direction of gradient vector g.

$$\therefore \quad \Delta x = -\lambda \frac{g}{|g|} \tag{2}$$

The optimum value of λ is found by univariate linear search in the direction $-\frac{g}{|g|}$.

This is called the steepest descent method. This method converges very slowly. The extension of this method is the conjugate gradient method. Assuming the objective function is quadratic of the form,

$$J(x) = \frac{1}{2} x'Gx + bx + c \tag{3}$$

one can find a sequence of search directions $u_1, u_2, \ldots, u_k$ such that

$$u_i \, Gu_j = 0 \qquad i \neq j \tag{4}$$

By moving sequentially in the directions $u_1, u_2, \ldots, u_k$ with linear univariate searches we can reach the optimum

$$X^*_{min} = X_0 + \sum_{i=1}^{n} \lambda_i \, u_i \tag{5}$$

The steepest descent and conjugate gradients are illustrated in Fig. 28 for two parameter case

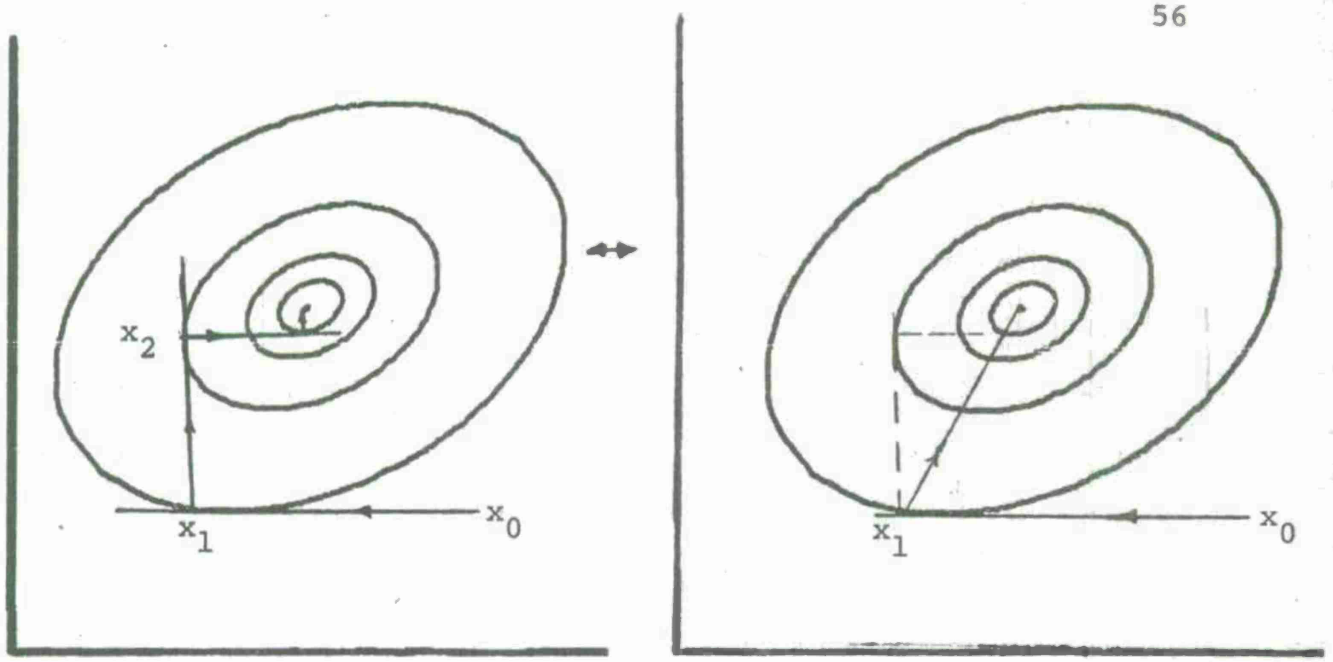

Steepest Descent

Conjugate Gradient

Figure 28a

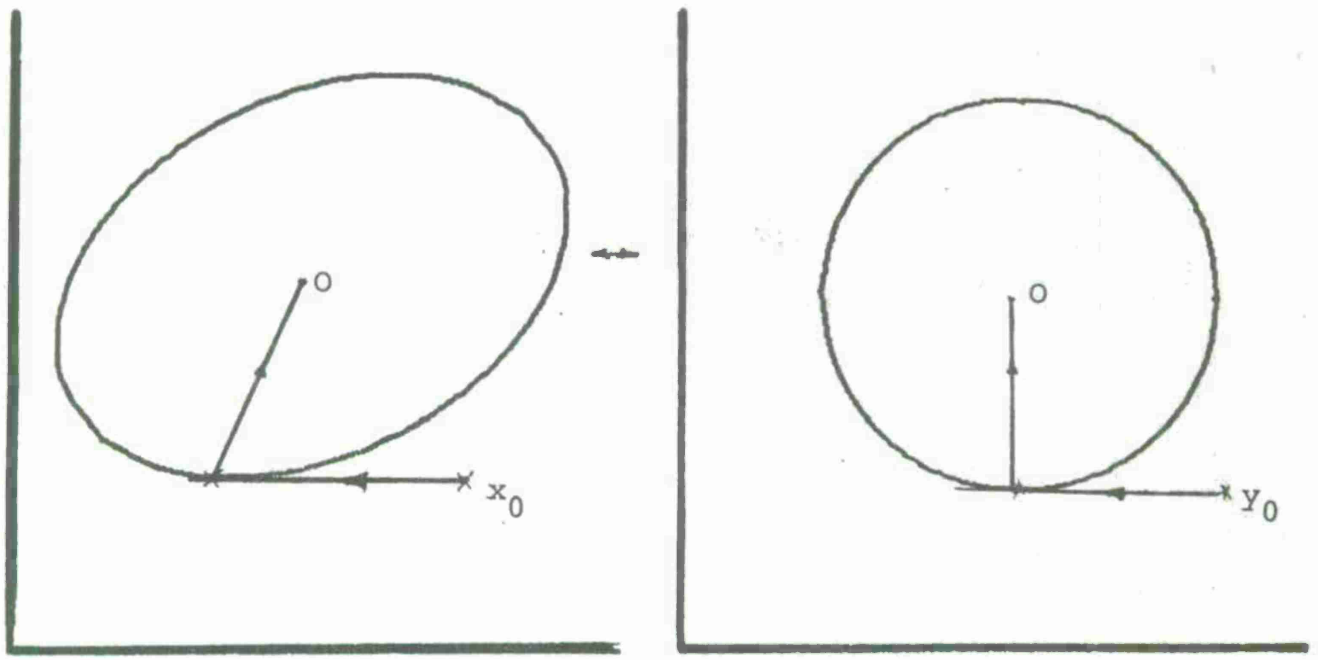

Figure 28b Concept of Conjugate Gradient

The conjugate gradient method transforms concentric elliptic contours into concentric circular contours. The circular contour has the desirable property of the normal to the tangent at any point passes through the center. Once the direction of normal is found in this plane, it can be transformed back to the original plane and direction of the increment in x can be found out and this will pass through the minimum for the quadratic function.

(3) Newton-Raphson Method

$$J(x+\Delta x) = J(x) + \Delta x'g + \frac{1}{2}\Delta x'G\,\Delta x \qquad (6)$$

differentiating with respect to Δx

$$\frac{\partial J(x+\Delta x)}{\partial \Delta x} = g + G\Delta x$$

for $x+\Delta x$ to be a optimum point

$$\frac{\partial J(x+\Delta x)}{\partial \Delta x} = 0$$

$$g + G\Delta x = 0 \quad , \quad \Delta x = -G^{-1}g \qquad (7)$$

This method is called Newton-Raphson and is a very efficient method if G and g are available.

The problem for non-quadratic function minimization is to find G which is positive definite and the question of how good an approximation of second order Taylor expansion is. The combination of conjugate gradient method for fast movement when away from minimum can be utilized with the conjugacy being with respect to the Hessian G. The Davidon-Fletcher-Powell (DFP) algorithm does exactly that.

The DFP algorithms continuously updates H, the inverse of the hessian matrix with linear search in direction of conjugate gradient by cubic interpolation. The step by step procedure given below is reproduced with variation from [4]. The details can be found in [2,3,4 & 5].

1) Set $H_1 = I$ and let k be the current iteration number, then set

$$d_k = -H_k g_k \tag{8}$$

then, d_k is the direction of search from the current point x_k

2) Perform a linear search to find $\lambda^*_k (>0)$, where λ^*_k is the value of λ_k that minimizes $J(x_k+\lambda_k b_k)$

3) Set $\Delta x_k = \lambda^*_k d_k$ (9)

4) Set $x_{k+1} = x_k + \Delta x_k$ (10)

giving the new current point

5) Evaluate $J(x_{k+1})$ and g_{k+1}

6) Set $\Delta g_k = g_{k+1} - g_k$ (11)

7) $$H_{k+1} = H_k + \frac{\Delta x_k \, \Delta x'_k}{\Delta x'_k \Delta g_k} + \frac{H_k \Delta g_k \Delta g'_k H_k}{\Delta' g_k H_k \Delta g_k}$$

8) Set k=k+1 and return to step 1.

9) Stop when either $|d_k|$ or every component of d_k is smaller than some prescribed amount.

The linear search in step 2 can be performed in two ways with cubic interpolation or golden section search.

Cubic interpolation procedure:

1) Evaluate $J_0 = J(x_k)$ and $G_0 = g_k' d_k$ (12)

check $G_0 < 0$. Compute α by

$$\alpha = \min[2, -\frac{2(J_0-J_e)}{G_0}] \quad (13)$$

where Je is the estimated values of $J(x_k+\lambda^*_k d_k)$.

2) Evaluate $J_\alpha = J(x_k+\alpha\, d_k)$ and $G_\alpha = g_\alpha = g' d_k$

3) If $G_\alpha > 0$ or if $J_\alpha > J_0$, proceed to rule 5 otherwise go to rule 4.

4) Replace α by 2α, return to rule 2.

5) Interpolate in the interval $[0,\alpha]$ for λ^*_k using

$$\frac{\lambda^*_k}{\alpha} = 1 - \frac{G_\alpha+w-Z}{G_\alpha-G_0+2w} \quad (14)$$

where

$$w = (z^2-G_0G_2)^{1/2} \quad (15)$$

and

$$Z = \frac{3}{\alpha}(J_0-J_\alpha) + G_0 + G_\alpha$$

6) Return to rule 5 to repeat the interpolation in the smaller interval $[0,\lambda^*_k]$ or $[\lambda_k,\alpha]$ accordingly as

$$g'_{k+1}\, d_k \gtrless 0 \text{ or } < 0$$

stop when the interval of interpolation has decreased to some prescribed value.

The complex method of M.J. Box [6], [7], with random search generates a simplex of n+1 points where n is the number of parameters to be optimized. The function is computed at each of the vertexes and the worst vertex is discarded. The reflection of this discarded vertex into the centroid of the remaining vertices is taken as a new vertex and search is carried out in two dimensions, the procedure is as follows:

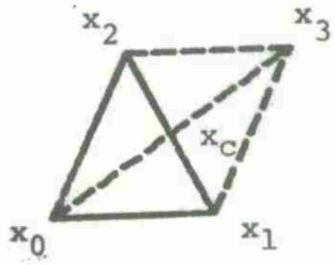

Three initial vertices are x_0, x_1, x_2. Let x_0 be the worst vertex and x_c be the centroid of x_1 and x_2. Then x_3 is computed by the relation

$$x_3 = (1+\alpha)x_c - \alpha\, x_{min}$$

where x_{min} is vertex with minimum function value. The procedure is repeated until minimum is obtained.

Appendix III

Design Data for M-37 Recoil Mechanism

M-37 recoil mechanism is designed for firing zone 7. All the pertinent parameters necessary for simulation of recoil mechanism model developed in Chapter 1 are given below. The variable area of the groove machined in the floating piston is tabulated in Table 2. Breech forces are tabulated in Tables 3 through 7 for zones 1, 5 through 8. These breech forces are simulated breech force data rather than actual test data. All the design data listed here was provided by Control and Stabilization group of General Rodman Laboratory, Army Weapons Command at Rock Island, Illinois.

m_R - Mass of recoiling parts = 3.6658 lbf sec^2/in

m_P - Mass of floating piston = .06735 lbf sec^2/in

ρ - Mass density of hydraulic fluid = .78E-4

P_0 - Initial gas pressure = 1153 psi

V_0 - Initial volume of gas = 513 in^3

R - Gas constant = 1.68

A_R - Recoil piston area = 2.9906 in^2

A_C - Control rod area = 2.4053 in^2

A_D - Floating piston area = 11.781 in^2

$C_1=C_2=C_3$ - Discharge coefficients = .8

A_1 - Area of orifice 1 = 1.25 in^2

A_2 - Area of orifice 2 = .4536 in^2

TABLE 2- AREA OF VARIABLE ORIFICE A3

X	A3(X)	X	A3(X)
0.00000	.08680	15.12600	.07900
.50420	.09370	15.63020	.07710
1.00840	.09410	16.13440	.07520
1.51260	.09630	16.63860	.07320
2.01680	.09950	17.14280	.07130
2.52100	.10110	17.64700	.06940
3.02520	.10210	18.15120	.06750
3.52940	.10250	18.65540	.06540
4.03360	.10270	19.15960	.06320
4.53780	.10290	19.66380	.06100
5.04200	.10280	20.16800	.05880
5.54620	.10250	20.67220	.05630
6.05040	.10190	21.17640	.05380
6.55460	.10120	21.68060	.05120
7.05880	.10060	22.18480	.04870
7.56300	.09960	22.68900	.04580
8.06720	.09870	23.19320	.04290
8.57140	.09770	23.69740	.03980
9.07560	.09670	24.20160	.03650
9.57980	.09540	24.70580	.03270
10.08400	.09410	25.21000	.02870
10.58820	.09290	25.71420	.02410
11.09240	.09150	26.21840	.01910
11.59660	.09000	26.72260	.01330
12.10080	.08850	27.22680	.00620
12.60500	.08720	27.73100	0.00000
13.10920	.08570	28.23520	0.00000
13.61340	.08410	28.73940	0.00000
14.11760	.08250	29.24360	0.00000
14.62180	.08090		

TABLE 3- BREECH FORCE FOR ZONE 1

T	B(T)	T	B(T)
0.00000	9.0	.03800	1757.0
.00050	5.0	.04000	1526.0
.00100	6.0	.04200	1329.0
.00150	7.0	.04400	1159.0
.00200	8.0	.04600	1013.0
.00250	9.0	.04800	887.0
.00300	10.0	.05000	778.0
.00350	11.0	.05200	683.0
.00400	12.0	.05400	602.0
.00450	10.0	.05600	530.0
.00500	72.0	.05800	468.0
.00550	1177.0	.06000	414.0
.00600	2041.0	.06200	367.0
.00650	3287.0	.06400	326.0
.00700	5272.0	.06600	289.0
.00750	8393.0	.06800	257.0
.00800	13220.0	.07000	229.0
.00850	20477.0	.07200	205.0
.00900	30924.0	.07400	183.0
.00950	44999.0	.07600	163.0
.01000	62189.0	.07800	146.0
.01050	80403.0	.08000	131.0
.01100	96098.0	.08200	118.0
.01150	105714.0	.08400	106.0
.01187	107588.0	.08600	95.0
.01250	102620.0	.08800	86.0
.01300	93260.0	.09000	77.0
.01350	82047.0	.09200	70.0
.01400	70792.0	.09400	63.0
.01450	60482.0	.09600	57.0
.01500	51500.0	.09800	52.0
.01550	43889.0	.10000	47.0
.01600	37532.0	.10200	43.0
.01650	32252.0	.10400	39.0
.01700	27872.0	.10600	35.0
.01750	24231.0	.10800	32.0
.01800	21192.0	.11000	29.0
.01850	18643.0	.11200	27.0
.01900	16493.0	.11400	24.0
.01950	14669.0	.11600	22.0
.02000	13113.0	.11800	20.0
.02050	11778.0	.12000	19.0
.02100	10626.0	.12200	17.0
.02150	9626.0	.12400	16.0
.02200	8755.0	.12600	14.0
.02250	7992.0	.12800	13.0
.02300	7320.0	.13000	12.0
.02350	9726.0	.13200	11.0
.02400	6199.0	.13400	10.0
.02450	5729.0	.13600	9.0
.02500	5309.0	.13800	9.0
.02550	4933.0	.14000	8.0
.02600	4593.0	.14200	7.0
.02650	4286.0	.14400	7.0
.02700	4009.0	.14600	6.0
.02724	3884.0	.14800	6.0
.02750	3808.0	.15000	5.0
.02800	3665.0	.15200	5.0
.03000	3149.0	.20000	0.0
.03200	2712.0		
.03400	2342.0		
.03600	2026.0		

TABLE 4- BREECH FORCE FOR ZONE 5

T	B(T)	T	B(T)
0.00000	159.0	.03600	2426.0
.00050	246.0	.03800	2069.0
.00100	513.0	.04000	1769.0
.00150	938.0	.04200	1517.0
.00200	1724.0	.04400	1304.0
.00250	3118.0	.04600	1123.0
.00300	5642.0	.04800	969.0
.00350	10127.0	.05000	839.0
.00400	18001.0	.05200	727.0
.00450	31434.0	.05400	632.0
.00500	53257.0	.05600	550.0
.00500	85873.0	.05800	480.0
.00600	128386.0	.06000	419.0
.00650	173036.0	.06200	367.0
.00700	206142.0	.06400	322.0
.00748	217035.0	.06600	283.0
.00750	217008.0	.06800	249.0
.00800	205962.0	.07000	220.0
.00850	181687.0	.07200	194.0
.00900	153385.0	.07400	172.0
.00950	126693.0	.07600	152.0
.01000	103872.0	.07800	135.0
.01050	85258.0	.08000	120.0
.01100	70386.0	.08200	107.0
.01200	49196.0	.08400	95.0
.01250	41695.0	.08600	85.0
.01300	35654.0	.08800	76.0
.01350	30747.0	.09000	68.0
.01400	26725.0	.09200	61.0
.01450	23400.0	.09400	54.0
.01500	20628.0	.09600	49.0
.01550	18298.0	.09800	44.0
.01600	16324.0	.10000	39.0
.01650	14641.0	.10200	36.0
.01700	13195.0	.10400	32.0
.01734	12315.0	.10600	29.0
.01750	12135.0	.10800	26.0
.01800	11575.0	.11000	24.0
.02000	9605.0	.11200	21.0
.02200	7998.0	.11400	19.0
.02400	6683.0	.11600	18.0
.02600	5602.0	.11800	16.0
.02800	4711.0	.20000	0.0
.03000	3973.0		
.03200	3361.0		
.03400	2852.0		

TABLE 5 - BREECH FORCE FOR ZONE 6

T	B(T)	T	B(T)
0.00000	384.0	.03500	2545.0
.00050	706.0	.03700	2135.0
.00100	1491.0	.03900	1797.0
.00150	2937.0	.04100	1517.0
.00200	5800.0	.04300	1285.0
.00250	11343.0	.04500	1091.0
.00300	21947.0	.04700	929.0
.00350	41614.0	.04900	793.0
.00400	76017.0	.05100	678.0
.00450	130033.0	.05300	582.0
.00500	200301.0	.05500	500.0
.00550	267029.0	.05700	431.0
.00600	302300.0	.05900	373.0
.00616	304395.0	.06100	323.0
.00650	295349.0	.06300	280.0
.00700	259560.0	.06500	243.0
.00750	214473.0	.06700	212.0
.00800	172277.0	.06900	185.0
.00850	137329.0	.07100	162.0
.00900	109863.0	.07300	142.0
.00950	88691.0	.07500	124.0
.01000	72415.0	.07700	109.0
.01050	59835.0	.07900	96.0
.01100	50018.0	.08100	85.0
.01150	42274.0	.08300	75.0
.01400	20888.0	.08500	66.0
.01431	19380.0	.08700	59.0
.01450	18986.0	.08900	52.0
.01500	17983.0	.09100	46.0
.01700	14514.0	.09300	41.0
.01900	11769.0	.09500	37.0
.02100	9586.0	.09700	33.0
.02300	7841.0	.09900	29.0
.02500	6440.0	.10100	26.0
.02700	5310.0	.10300	24.0
.02900	4395.0	.20000	0.0
.03100	3651.0		
.03300	3043.0		

TABLE 6- BREECH FORCE FOR ZONE 7

T	B(T)	T	B(T)
0.00000	2809.6	.01700	13971.0
.00020	4589.6	.01740	13354.0
.00060	9058.6	.01780	12765.0
.00100	18069.0	.01820	12204.0
.00140	35565.0	.01860	11668.0
.00180	68543.0	.01900	11156.0
.00220	126940.0	.01940	10674.0
.00260	219070.0	.01980	10214.0
.00300	337720.0	.02020	9775.1
.00340	446170.0	.02060	9355.5
.00380	496900.0	.02100	8954.5
.00420	476070.0	.02140	8576.1
.00460	411400.0	.02180	8215.1
.00500	335660.0	.02220	7869.6
.00540	267300.0	.02226	7538.8
.00580	211870.0	.02300	7222.5
.00620	168900.0	.02340	6924.1
.00660	136050.0	.02380	6638.1
.00700	110950.0	.02420	6364.5
.00740	91613.0	.02460	6102.9
.00780	76562.0	.02500	5852.1
.00820	64706.0	.02540	5615.3
.00860	55253.0	.02580	5389.0
.00900	47627.0	.02620	5171.7
.00940	41322.0	.02660	4963.0
.00980	36281.0	.02700	4763.3
.01020	32030.0	.02740	4574.0
.01060	29784.0	.02780	4393.7
.01100	28358.0	.02820	4220.4
.01140	27013.0	.02860	4054.0
.01180	25736.0	.02900	3894.2
.01220	24521.0	.02940	3743.0
.01260	23366.0	.02980	3598.0
.01300	22268.0	.03020	3458.6
.01340	21237.0	.04020	1361.8
.01380	20257.0	.05020	578.4
.01420	19324.0	.06020	263.3
.01460	18435.0	.07020	128.1
.01500	17588.0	.08020	63.5
.01540	16794.0	.09020	0.0
.01580	16036.0	.20000	0.0
.01620	15314.0		
.01660	14626.0		

TABLE 7 - BREECH FORCE FOR ZONE 8

T	B(T)	T	B(T)
0.00000	3090.6	.01700	15368.1
.00020	5048.6	.01740	14689.4
.00060	9964.5	.01780	14041.5
.00100	19875.9	.01820	13424.4
.00140	39121.5	.01860	12834.8
.00180	75397.3	.01900	12271.6
.00220	139634.0	.01940	11741.4
.00260	240977.0	.01980	11235.4
.00300	371491.9	.02020	10752.6
.00340	490786.9	.02060	10291.0
.00380	546589.9	.02100	9849.9
.00420	523676.9	.02140	9433.7
.00460	452539.9	.02180	9036.6
.00500	369225.9	.02220	8656.6
.00540	294029.9	.02226	8292.7
.00580	233057.0	.02300	7944.7
.00620	185790.0	.02340	7616.5
.00660	149655.0	.02380	7301.9
.00700	122045.0	.02420	7000.9
.00740	100774.3	.02460	6713.2
.00780	84218.2	.02500	6437.3
.00820	71176.6	.02540	6176.8
.00860	60778.3	.02580	5927.9
.00900	52389.7	.02620	5688.9
.00940	45454.2	.02660	5459.3
.00980	39909.1	.02700	5239.6
.01020	35233.0	.02740	5021.4
.01060	32762.4	.02780	4833.1
.01100	31193.8	.02820	4642.4
.01140	29714.3	.02860	4459.4
.01180	28309.6	.02900	4283.6
.01220	26973.1	.02940	4117.3
.01260	25702.6	.02980	3957.8
.01300	24494.8	.03020	3804.5
.01340	23360.7	.04020	1458.0
.01380	22282.7	.05020	636.2
.01420	21256.4	.06020	289.6
.01460	20278.5	.07020	140.9
.01500	19346.8	.08020	69.8
.01540	18473.4	.09020	0.0
.01580	17639.6	.20000	0.0
.01620	16845.4		
.01660	16088.6		

DISTRIBUTION

	Copies
Defense Documentation Center ATTN: TIPCR Cameron Station Alexandria, VA 22314	12
Commander US Army Harry Diamond Laboratories ATTN: AMXDO-EDC AMXDO-SA Washington, DC 20438	1 1
Commander US Army Armament Materiel Readiness Command ATTN: DRSAR-LEM Rock Island, IL 61201	1
Commander US Army Armament Research & Development Command ATTN: DRDAR-LCW Mr. R. Wrenn DRDAR-LCW Mr. M. Barran DRDAR-SCW-T Mr. E. Larrison Picatinny Arsenal Dover, NJ 07801	 1 1 1
Commander US Army Research Office ATTN: Information Processing Office P.O. Box 12211 Research Triangle Park, NC 27709	1
Commander US Army Tank-Automotive Research & Development Command ATTN: Technical Library DRCPM-60 Warren, MI 48090	1 1
Commander Project Manager Cannon Artillery Weapons Systems ATTN: DRCPM-CAWS Dover, NJ 07801	1

Commander
Rock Island Arsenal
ATTN: SARRI-ENW 10
SARRI-EN 1
SARRI-ADL 2
Rock Island, IL 61201

University of Wisconsin-Madison
Department of Mechanical Engineering
ATTN: Dr. S. Wu 5
Madison, WI 53706